

CO₂ Mineralization Using Reactive Species

Juan Ma

Thesis submitted to the faculty of the
Virginia Polytechnic Institute and State University
in partial fulfillment of the requirements for the degree of

Master of Science

In

Mining and Minerals Engineering

Roe-Hoan Yoon, Committee chair

Gregory T. Adel

Gerald H. Lutrell

April 24, 2012

Blacksburg, Virginia

Keywords: CO₂ sequestration, mineralization, reactive cations, nesquehonite, kinetics

Copyright 2012, Juan Ma

CO₂ Mineralization Using Reactive Species

Juan Ma

ABSTRACT

To address the environmental changes associated with increasing levels of atmospheric CO₂, a possibility of mineralizing CO₂ with the species such as Ca²⁺ and Mg²⁺ ions that are already present in sea water was studied. A series of experiments conducted at temperatures in the range of 20 to 40°C showed that the activation energy for the formation of nesquehonite (MgCO₃·3H₂O) is 64.6 kJ/mol. It was found that the activation energy barrier can be readily overcome by simple agitation and heating at slightly elevated temperatures, *e.g.*, 40°C. The kinetics of mineralization and the %Mg²⁺ ion utilization varies depending on energy dissipation rate, temperature, pH, and NaCl concentration. The maximum Mg²⁺ ion utilization achieved was 86%. Thermodynamic calculations were carried out to construct the species distribution diagrams, predict the pH of CO₂ mineralization, and to predict %Mg ion utilization (or extraction) from sea water.

To address the issues concerning the acidification of sea water during CO₂ mineralization, spent solutions were treated with basic minerals such as limestone and olivine. It was found that in the presence of these minerals the pH rises to the pH of minimum solubility of the buffering mineral. The pH of minimum solubility of limestone is 8.3 and that of olivine is 8.6. Other means of pH neutralization were also discussed.

Acknowledgements

My most sincere gratitude goes to my dear advisor, Dr. Roe-Hoan Yoon, for his support and guidance throughout the course of my master's program; for his inspiration, suggestion, and encouragement in my research; and for his sharing of his philosophy and life lessons.

Sincere thanks are also directed to Dr. Gerald H. Luttrell and Dr. Gregory T. Adel for serving on my committee and for their kindness and valuable suggestions.

Especially, I thank Dr. Neil E. Johnson in Department of Geosciences. He is very nice and provided the XRD measurements for my research. I also thank him for his analysis of the XRD patterns and useful discussion.

My thanks also go to Thomas P. Wertalik in Glass Shop in Department of Chemistry and Stephen McCartney in Nanoscale Characterization and Fabrication Laboratory (NCFL) for their great technical support.

Funding for this project was provided by U.S. Department of Energy, whom I sincerely thank.

I want to extend my thanks to the past and present fellows and staffs at the Center for Advanced Separation Technologies (CAST), particularly, Jinming Zhang, Jialin Wang, Ruijia Wang, Jing Niu, Christopher E. Hull, Kirsten Titland, and Kathy Flint for their support and friendship. Many thanks go to Lei Pan and Zuoli Li for their precious advice and help in both my research and life and for their friendship. I also thank Yihong Yang for teaching me to measure bubble-particle interaction and for his suggestions.

Finally, I would like to express my eternal gratitude to my parents, for their unconditional love and support.

Table of contents

Chapter 1 Introduction	1
1.1 General	1
1.2 Literature Review	3
1.2.1 Geological sequestration	3
1.2.2 Ex situ CO ₂ mineralization using minerals	5
1.2.2.1 Direct dry carbonation at high temperature	6
1.2.2.2 HCl extraction route.....	6
1.2.2.3 Direct aqueous mineral carbonation	7
1.2.3 Ex situ CO ₂ mineralization using reactive species	9
1.2.3.1 Sources of reactive cations.....	9
1.2.3.2 Previous studies on CO ₂ mineralization using cations	10
1.2.3.3 Present study of CO ₂ mineralization using reactive Mg ²⁺ and/or Ca ²⁺ ions.....	11
1.3 Thesis Outline.....	12
1.4 References	12
Chapter 2 CO₂ Mineralization Using Reactive Mg²⁺ Ions.....	16
2.1 Introduction	16
2.1.1 Nesquehonite	16
2.1.2 Chemical reaction.....	18
2.1.3 Saturation index.....	19
2.2 Thermodynamic Calculation by <i>Visual Minteq</i>	20
2.3 Experiment	23
2.3.1 Materials.....	23
2.3.2 Procedure.....	24
2.3.3 Standard EDTA titration	25
2.3.4 Characterization of the solid product	26
2.4 Results	26
2.5 Discussion	31

2.5.1 Ocean capacity	31
2.5.2 Other magnesium sources	32
2.5.3 Controlling pH.....	32
2.5.4 Advantages of the new approach.....	37
2.6 Conclusions	38
2.7 References	38
Chapter 3 A Kinetic Study of Nesquehonite Precipitation	41
3.1 Introduction	41
3.2 Theoretical approach	42
3.2.1 Chemical reactions	42
3.2.2 Kinetic model	42
3.2.3 The temperature dependence of rate constants.....	42
3.3 Experiment	42
3.4 Results and discussion.....	43
3.4.1 Effect of stirring speed	43
3.4.2 Effect of aeration	44
3.4.3 Effect of NaCl additive.....	45
3.4.4 Effect of ultrasonic	46
3.4.5 Effect of temperature.....	47
3.4.6 Effect of pH	50
3.4.7 Characterization of solid products.....	52
3.5 Conclusions	53
3.6 References	54
Chapter 4 CO₂ Mineralization Using Ca²⁺ Ions Alone and Using Mg²⁺ and Ca²⁺ Ions Together	56
4.1 Introduction	56
4.1.1 CO ₂ mineralization using Ca ²⁺ ions alone.....	56
4.1.2 CO ₂ mineralization using Mg ²⁺ and Ca ²⁺ ions together	57

4.1.3 Chemical reaction.....	57
4.2 Experiment	58
4.2.1 Materials.....	58
4.2.2 Procedure.....	58
4.3 Results and Discussion.....	59
4.3.1 CO ₂ mineralization using Ca ²⁺ ions alone.....	59
4.3.2 CO ₂ mineralization using Mg ²⁺ and Ca ²⁺ ions together	60
4.4 Conclusions	62
4.5 References	62
Chapter 5 Conclusions and Future Work.....	63
5.1 Conclusions	63
5.2 Future Work	64

List of figures

Figure 2.1	Carbonic species distribution in CO ₂ -H ₂ O system at different pH levels at 22 °C..	20
Figure 2.2	Carbonic species concentrations in CO ₂ -H ₂ O system at different equilibrium pH levels at 22 °C based on infinite CO ₂ gas at atmospheric CO ₂ pressure. Dashed line represents the total concentration of carbonic species.	21
Figure 2.3	Mg-species concentrations in CO ₂ -Mg ²⁺ -H ₂ O system at different pH levels at 22 °C.	22
Figure 2.4	SI-pH diagram for different Mg-carbonate minerals at 22 °C.	23
Figure 2.5	Schematics of the experimental set-up. (a): the set-up used in step 1; (b): the set-up used in step 2.	25
Figure 2.6	Changes in Mg ²⁺ ion concentration ([Mg ²⁺]), reduction of [Mg ²⁺] and pH of the solution during nesquehonite formation.....	27
Figure 2.7	XRD pattern of the precipitated solid product compared with a reference XRD spectra of nesquehonite (red dots).....	28
Figure 2.8	SEM images of the precipitated solid product.....	29
Figure 2.9	EDS analysis of the precipitated solid product.....	30
Figure 2.10	Conceptual flowsheet of the process of CO ₂ mineralization using reactive Mg ²⁺ /Ca ²⁺ ions.	32
Figure 2.11	Solubility diagram of limestone at 25 °C and atmospheric CO ₂ partial pressure. The dashed line represents the concentration of total dissolved species.	35
Figure 2.12	Changes in the solution pH in the presence of limestone with and without injecting CO ₂ at 25 °C.....	35
Figure 2.13	Solubility diagram of forsterite at 25 °C and atmospheric CO ₂ partial pressure. The dashed line represents the concentration of total dissolved species.	36
Figure 2.14	Changes in the solution pH in the presence of olivine with and without injecting CO ₂ at 25 °C.....	36

Figure 3.1	The effect of stirring speed on nesquehonite precipitation.....	43
Figure 3.2	The effect of aeration on nesquehonite precipitation.	44
Figure 3.3	The effect of NaCl on nesquehonite precipitation.....	45
Figure 3.4	The effect of ultrasonic on nesquehonite precipitation.	46
Figure 3.5	The first-order kinetic plots for nesquehonite precipitation at 20, 30, 40 °C.....	47
Figure 3.6	Measured Mg ²⁺ ion concentration data and first-order model data during nesquehonite precipitation at 20, 30, 40 °C. The solid lines represent modelling data at corresponding temperature using Equation [3-2].....	48
Figure 3.7	Arrhenius plot for nesquehonite precipitation.....	49
Figure 3.8	pH effect on nesquehonite precipitation.....	50
Figure 3.9	% Reduction of Mg ²⁺ ion at different pHs at reaction times of 30 min and 1 h.....	51
Figure 3.10	XRD pattern of the solid products under different experimental conditions. (a) 20 °C, pH 6.9; (b) 30 °C, pH 6.9; (c) 40 °C, pH 6.9; (d) 40 °C, pH 6.6; (e) 40 °C, pH 7.2; (f) 40 °C, pH 7.5.....	53
Figure 4.1	Change in the sum of Mg ²⁺ and Ca ²⁺ ion concentration during the precipitation of solid products.....	60
Figure 4.2	The XRD pattern of the solid product.....	61

List of tables

Table 1.1 Mg ²⁺ and Ca ²⁺ ion concentrations (mg/L) in seawater and brines	10
Table 4.1 The Gibbs free energy of the formation of selected Ca/Mg-carbonate.....	57
Table 4.2 Radius, cation-O distance and water binding energy for Mg/Ca complex	59
Table 4.3 Solubility product of selected calcium/magnesium mineral	60

Chapter 1

Introduction

1.1 General

Since the mid-20th century, widespread environmental changes associated with global warming have drawn the attention of global scientists from a variety of disciplines¹⁻⁵. For example, the potential effects of climate change on water resources, ecosystems, coastal management, agriculture, industries, and many other areas⁵ have prompted academic, governmental, and industrial researchers to investigate a variety of possible strategies and technologies for reducing global warming. Additionally, several high-profile international collaborative programs, such as the Intergovernmental Panel on Climate Change (IPCC), the United Nations Framework Commission on Climate Change, and the Global Climate Change Initiative⁶ are also addressing this complex and potentially far-reaching problem.

One of the acknowledged causes for global warming is the emission of increased anthropogenic green house gases (GHG) into the atmosphere^{5,7}, which scientists believe must be reduced if this problem is to be addressed realistically. There are four long-lived GHGs: carbon dioxide (CO₂), methane (CH₄), nitrous oxide (N₂O) and halocarbons (a group of gases containing fluorine, chlorine or bromine)⁵. Among these GHGs, CO₂ is by far the largest contributor, accounting for 76.7 percent of the total global anthropogenic GHG emission into the atmosphere⁵. Therefore, the present study focuses on reducing CO₂ emissions.

CO₂ emissions—and thus atmospheric CO₂ concentrations—have been increasing for decades. Globally, annual CO₂ emissions were in the range of 15 Gt in 1970; that figure nearly doubled to ~28 Gt in 2004⁵. In the United States, annual CO₂ emissions were 5.1 Gt in 1990, increasing to 5.5 Gt in 2009⁷. A 1996 study of CO₂ concentration in Antarctic ice core samples produced some compelling findings⁸. During the preindustrial period (defined as the period prior to 1800), actual CO₂ concentrations in the atmosphere remained constant at about 280 ppmv; a sample linked to the mid-1950s, however, showed CO₂ concentrations at 315 ppmv in 1958. And 2008 data obtained in Hawaii documented further increases—to 385 ppmv⁹. Without significant changes in energy policies and related technologies, CO₂ emissions will continue to increase. In fact, the Energy Information Administration (EIA) in the U.S. predicts that 2035, approximately

42.4 Gt of CO₂ will be emitted into the atmosphere¹⁰. Thus, the need to reduce CO₂ emissions is urgent.

Generally, three options can be applied to achieve this goal^{11,12}. The first is to reduce energy intensity, which requires efficient conversion and use of energy so that fewer fossil fuels—the largest source of CO₂ emission—are required to provide the same energy service. The second option is to reduce carbon intensity, which necessitates the use of a number of alternative low- or no-carbon energies (solar, wind, wave, tidal, geothermal, hydroelectric energy, etc.⁴). The third option is to improve the sequestration of CO₂, which involves CO₂ capture and storage (CCS) to prevent carbon emissions from reaching the atmosphere. While widespread investigations involving efficiency improvements and the move toward alternative energy sources are ongoing, CCS has received much less attention to date.

Nonetheless, the sequestration of CO₂ is important and necessary for a number of reasons and should be included in a three-pronged approach to reducing CO₂ emissions. First, reducing energy intensity alone may not satisfy expected energy demands, which will no doubt increase with continued industrialization, especially in fast-developing countries such as China and India¹⁰. Second, it is presently impractical to replace well established and relatively low-cost fossil-fuel technologies with any of the newer technologies noted because they are costly and are not currently capable of satisfying the world's energy needs¹³. In addition, fossil fuels (coal, petroleum, and natural gas) have other advantages such as their widespread availability and their ease of transport. These plusses mean that fossil fuels are likely to continue to be the primary energy source in the coming decades, at least for the remainder of this century¹¹. This likelihood reinforces the need for additional research on CO₂ sequestration, which can help to serve as a “green bridge” between the fossil-fuel-fired energy systems now in use to the low- or no-carbon energy systems of the future.

As noted, the sequestration of CO₂ necessitates the capture and storage of this greenhouse gas, which is produced by the combustion of fossil fuels used in power plants and other industrial facilities (e.g., oil refineries and iron, steel, and cement production plants), before it is released into the atmosphere¹¹. Once captured, the CO₂ can be compressed into a liquid, a superliquid or a gas stream and then transported by pipeline and injected into underground geological sites or into the ocean. Scientists and engineers are also looking into ways that it can

be directly converted into environmentally benign and stable products via biological and chemical processes.

A great many technologies have been studied to sequester anthropogenic CO₂, including oceanic, terrestrial, geological, biological and chemical options^{6,12,14-30}. Among these technologies, a relatively little-known approach—ex situ CO₂ mineralization using reactive cations—is both attractive and promising. Therefore, the objective of the present work is to study ex situ CO₂ mineralization using reactive Mg²⁺ and/or Ca²⁺ ions as an alternative of CO₂ sequestration. Both the thermodynamic and kinetic studies will be conducted.

1.2 Literature Review

This literature review encompasses three sections. First, a review of current CO₂ sequestration technologies used in industry provides a good reference for the proposed new approach. Second, available research on ex situ mineralization of CO₂ for sequestration will be assessed, with a particular focus on the strengths and limitations of the various applied methodologies. Third, the few studies that do exist with respect to ex situ CO₂ mineralization using reactive cations will be evaluated, and the resulting knowledge will inspire and direct the current effort.

1.2.1 Geological sequestration

Although there have been a number of investigations on the sequestration of CO₂, none of them have proven to be suitable for large-scale applications—with the exception of geological sequestration³¹. This process involves injecting CO₂ into the deep subsurface of the earth for long-term storage. After the CO₂ has been captured from fossil fuel combustion, it is transported to geological sites such as underground caverns or mines, porous and permeable rocks, oil or gas sites, unminable coal beds, and deep saline aquifers, and then injected into underground. Geological sequestration has been taking place on a large scale since 1996 at Sleipner West, a natural gas field off the coast of Norway. Statoil, the operators of the Sleipner field, uses an amine solvent to capture the excess CO₂ and then injects the separated CO₂ into an aquifer 1000 meters below the surface of the North Sea where it is stored³². Approximately one million tons of CO₂ are sequestered annually, thereby preventing it from entering the atmosphere³².

Three principal mechanisms can be used for CO₂ sequestration in geological formations¹¹. In the first mechanism, commonly referred to as the hydrodynamic trapping mechanism, CO₂ is trapped under a low-permeability caprock as a gas or supercritical fluid. The second mechanism, widely considered to be the most permanent and secure form of geological storage, is known as the solubility trapping mechanism. In this process, CO₂ is dissolved into the fluid phase, e.g., in petroleum. In the third mechanism, the mineral trapping mechanism, CO₂ can react either directly or indirectly with minerals and organic matter in geologic formations to form stable solid minerals such as calcium, magnesium, and iron carbonates. Mineral trapping is also referred to as in situ mineralization because it occurs underground at a very slow rate without displacing any existing rock material.

Despite its known advantages, e.g., it is commercially viable and can process a large capacity of CO₂, geological sequestration has some important challenges to overcome. The most important issue is the safety and security of underground CO₂ storage areas since the gas has the potential to leak from storage sites along permeable pathways to the near-surface environment³³. Even though the actual physical risks associated with leakage are still unclear, a CO₂-rich ground surface can pose significant risks. The most tragic example to date may be the Lake Nyos event³⁴⁻³⁶. During the night of August 21, 1986, a huge volume of naturally sequestered CO₂ was emitted from the Lake Nyos crater in Cameroon. The CO₂ gas reached 120 meters above the lake surface due to its lethal concentration. This disaster killed more than 1700 people and all animal life as far as 14 kilometers away from the crater. It is believed that a slow leak of CO₂ into the 220-meter deep lake from below oversaturated the water and caused the sudden and deadly release of CO₂. Currently, some approaches (e.g., well closure and abandonment) represent short-term measures for avoiding the risks associated with excess surface CO₂ at open sites. However, according to Ide³⁷, CO₂ leakage from wells, which can result from poor cementation, inadequate plugging techniques, overpressure, corrosion, and other failure-producing conditions, remains an unacceptable risk factor for CCS development projects.

Another problem associated with geological sequestration is leaching. Because CO₂ is an acidic gas, when it is injected into underground formations it can form high-pressure acidified brine, which has the potential to dissolve minerals, thereby increasing pore volume. Should this occur, it could breach the flow barriers on which sequestration relies and leach heavy metals out of mineral rock, thereby posing a long-term threat of transporting heavy metals to the closer

surface of freshwater aquifers¹⁶. These are important concerns for scientists and engineers, since geological sequestration technology must comply with the health-related standards designed to protect underground sources of drinking water mandated by the Safe Drinking Water Act (SDWA).

In summary, the potential for leakage and leaching problems associated with CO₂ sequestration in geological formations raise significant public concerns that must be addressed. Therefore, effective methods to monitor, detect, characterize, mitigate, and remediate CO₂ leakage and heavy metal leaching from geologic storage sites are essential if this technology is to be widely adopted by scientists, governments and communities at large.

1.2.2 Ex situ CO₂ mineralization using minerals

The safety and environmental issues associated with geological sequestration discussed above point to the need for more viable, ecologically responsible technologies. One with attractive potential is ex situ CO₂ mineralization—particularly in situations where geological sequestration is not feasible. The most attractive aspect of this method is that mineralization is, to date, the only environmentally benign, permanent process for storing CO₂ that eliminates the need for safety monitoring³⁸. In addition, minerals used in this process are found in large amounts in nature as components of ophiolite complexes^{39,40}, which are believed to exist in quantities that far exceed known supplies of fossil fuels⁴¹. Plus, the reactions involved in CO₂ mineralization are exothermic⁴²⁻⁴⁴, meaning that the process is a net energy producer.

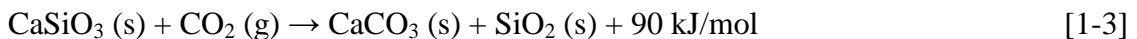
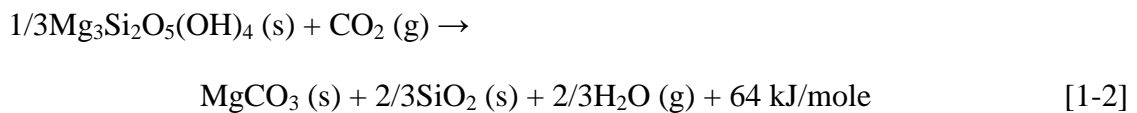
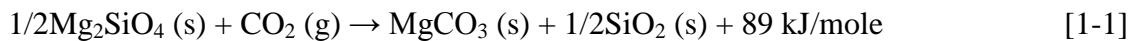
Here, we summarize previous studies on ex situ CO₂ mineralization using naturally occurring basic minerals, such as olivine and serpentine (CO₂ mineralization using reactive cations will be discussed later). To reiterate, in situ mineralization of CO₂ occurs underground via geological sequestration based on the mineral trapping mechanism, while the CO₂ mineralization processes outlined below are all above ground and ex situ.

The idea of CO₂ mineralization was first proposed by Seifritz in 1990⁴⁵. He proposed that the naturally occurring process of rock weathering could be mimicked to sequester CO₂. During the weathering process, CO₂ dissolves in water and reacts with basic silicate minerals, forming thermodynamically stable carbonates in a solid form⁴⁶. However, the natural weathering process tends to be extremely slow. In response, different process routes associated with CO₂

mineralization were studied to speed up the carbonation reaction in order to make the process economically viable. Listed below are the main routes studied.

1.2.2.1 Direct dry carbonation at high temperature

Lackner et al.⁴¹ were the first to conduct significant studies on CO₂ mineralization at the Los Alamos National Laboratory (LANL) in 1995. They firstly studied the simplest method, direct dry carbonation, where gaseous CO₂ directly reacts with basic minerals like forsterite, serpentine and wollastonite, as shown in equations [1-1], [1-2] and [1-3], respectively⁴⁷. The researchers showed that although the reaction proceeds very slowly at room temperature, it could be accelerated at higher temperatures. However, at a high temperature threshold, which varied according to the studied mineral, a shift in chemical equilibrium would occur, whereby free CO₂ was favored over the bound form. Therefore, increasing the temperature to speed up the reaction presented some inherent limitations. Moreover, even at elevated temperatures, the reaction was still too slow. Specifically, experiments conducted at temperatures of 140-300 °C, at a CO₂ pressure of 0.78bar, and using ground minerals with a grain size of 50 to 100 μm didn't show significant results even over the course of several days⁴⁸. Even when the CO₂ pressure was increased to 340 bar, only 30% of serpentinite was carbonated⁴⁸.



1.2.2.2 HCl extraction route

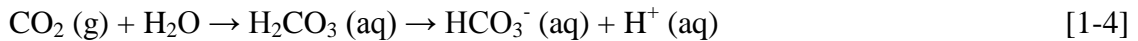
After repeated attempts to achieve dry carbonation of silicate minerals resulted in unacceptably slow kinetics, the LANL group studied a well known aqueous route to extract a more reactive form of magnesium, magnesium hydroxide (Mg(OH)₂), from natural minerals using hydrochloric acid (HCl)^{41,48}. Specifically, hydrochloric acid was initially used to dissolve specific minerals, e.g., forsterite and serpentinite, which was then recovered by heating the solution from 100 to 250 °C in a series of steps. The recovery step produces Mg(OH)₂ that reacts with gaseous CO₂ in a reactor at high temperature and pressure.

The HCl extraction route succeeded in improving carbonation kinetics. However, according to studies by Wendt et al.⁴⁹, the energy costs associated with the dehydration step needed for HCl recovery is too high for this route to be widely implemented. In fact, in related feasibility studies conducted by the National Energy Technology Laboratory (NETL) and the International Energy Agency (IEA), the energy required for the dehydration and crystallization steps was four times the amount of electrical energy produced by burning the coal^{50,51}. This differential makes the HCl process entirely too energy intensive.

1.2.2.3 Direct aqueous mineral carbonation

An alternative process for CO₂ mineralization is the direct aqueous mineral carbonation route, in which CO₂ reacts with fine particle-sized minerals in suspension in an autoclave at high temperature and high CO₂ pressure. NETL's Albany Research Center (ARC) initiated this research in 1998 and until fairly recently has devoted significant effort and resources conducting feasibility studies under the sponsorship of the U.S. Department of Energy (DOE).

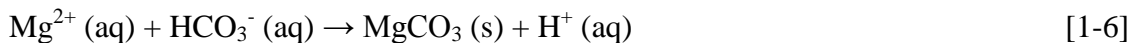
In the process of direct aqueous mineral carbonation, first, CO₂ dissolves in water and dissociates to HCO₃⁻ and H⁺ ions at high CO₂ pressure⁵², as shown in Reaction [1-4]:



Then the mineral is hydrolyzed by H⁺ ion, liberating Mg²⁺ ion and forming silicic acid or free silica and water, as shown in Reaction [1-5]:

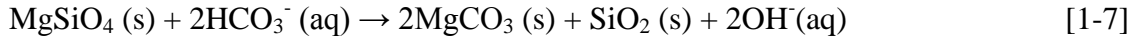


Finally, the Mg²⁺ ion reacts with HCO₃⁻ ion, forming the solid carbonate, as shown in Reaction [1-6]:



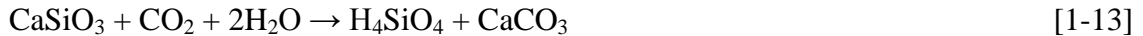
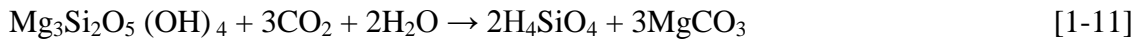
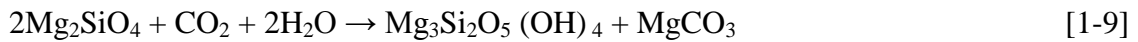
O'Connor et al.⁵² found that the addition of NaHCO₃ and NaCl into the solution could dramatically improve the carbonation reaction rate. The NaHCO₃/NaCl mixture produces a buffer that keeps the solution pH constant in the range of 7.7—8.0. Moreover, the added salt Cl⁻ ion improves the solubility of the mineral by forming several intermediate soluble complexes with magnesium, such as MgCl₂, MgCl₃⁻ and MgCl₄⁻, which increases the release of Mg²⁺ ion from the mineral.

For the modified solution, the reactions are as follows:



The HCO_3^- ion consumed in Reaction [1-7] is immediately regenerated by Reaction [1-8] between OH^- ion and CO_2 being injected into the solution, keeping the solution chemistry relatively constant. Therefore, the added HCO_3^- ion is believed to act as a catalyst rather than being consumed in the reaction⁵².

NETL-ARC first studied Mg-rich minerals, such as serpentine and olivine, due to their large abundance in nature⁵²⁻⁵⁴. Later, their experimental work demonstrated that in addition to Mg-bearing silicates, Ca- and Fe-bearing silicates also showed potential as possible reactants^{55,56}. Theoretical carbonation reactions of these silicates are shown below.



Activation of silicate minerals prior to carbonation can significantly improve the reaction rate, resulting in up to 80% stoichiometric conversion of the silicate to the carbonate within 30 minutes⁵⁴. Grinding and heating were found to be good methods for activating silicate minerals. Specifically, mined ores must be crushed and then ground to minus 75 μm or minus 38 μm using laboratory rod or ball mills. Finer particles could be achieved through the use of a stirred-media detritor (SMD). For serpentine, a heat pretreatment that removes the chemically bonded water from the mineral is also required. Ground samples were typically heated to 630 °C for 2 h⁵⁵. Olivine and wollastonite require no heat pretreatment.

The energy required for the activation of minerals is substantial. The estimated energy for the initial crushing is $\sim 2 \text{ kW}\cdot\text{h}/\text{ton}$; for grinding ($-75 \mu\text{m}$), $\sim 11 \text{ kW}\cdot\text{h}/\text{ton}$; for further grinding ($-38 \mu\text{m}$), $\sim 70 \text{ kW}\cdot\text{h}/\text{ton}$; for SMD milling, $\sim 150 \text{ kW}\cdot\text{h}/\text{ton}$, for heating for serpentine, $\sim 300 \text{ kW}\cdot\text{h}/\text{ton}$ ⁵⁵.

In addition to the high energy costs associated with pretreatment, another problem is the large scale of mining. Direct aqueous mineral carbonation would require a massive amount of natural rocks, which would entail significant mining-related investments and expenditures. As estimated by Gerdemann⁵⁵, in order to sequester all of the CO₂ generated by burning coal, more than five times as much ore in comparison to the coal would need to be mined, which could end up being prohibitively large for actual industrial process. As an example, approximately 55,000 tons of mineral would be required for the daily mineral carbonation of the CO₂ emissions from a single 1-GW, coal-fired power plant⁵⁵.

Thus, the high-energy demands associated with essential pretreatment steps, as well as the large scale of mining operations to produce the needed ore, make the direct aqueous mineral carbonation route impractical. Nevertheless, this study provided valuable information, remains the current state-of-the-art, and is considered to be a starting point for future improvements.

1.2.3 *Ex situ CO₂ mineralization using reactive species*

Twenty years of research and development addressing CO₂ mineralization using silicate minerals has failed to produce a viable, economical technology that could be applied on a large-scale. Nevertheless, CO₂ mineralization has the unbeatable advantage of permanent and safe storage of CO₂ compared to geological sequestration, which is why it merits further R&D as a potential solution to the problem of carbon management. This study, therefore, proposes a relatively new approach of CO₂ mineralization, where reactive cations such as Mg²⁺, Ca²⁺, and Fe²⁺ ions are used in place of natural silicate minerals to react with gaseous CO₂ in an aqueous solution, forming thermodynamically stable solid carbonates.

As discussed above, the main limitation of CO₂ mineralization using silicate minerals is the high-energy cost required for their extraction and activation—which is why reactive ions are superior to silicate minerals since no extraction or activation is needed. Plus, the precipitation of the magnesium and calcium carbonates from Mg²⁺ and/or Ca²⁺ ions offers much faster kinetics in comparison to when the cations are bound in a silicate structure.

1.2.3.1 Sources of reactive cations

Possible sources of the essential reactive cations needed for ex situ CO₂ mineralization could be seawater, saline brines from oil and gas extraction, and calcium/magnesium-rich

wastewater. The world's oceans, potentially the greatest natural sinks for sequestration of anthropogenic CO₂ emissions, contains high levels of Mg²⁺ and Ca²⁺ ions. Additionally, condensed seawater from desalination plants contains higher concentrations of these two cations. Also, produced water contains high concentration of the mentioned two cations. Currently, twenty to thirty billion barrels of saline-produced water are generated annually in the oil and gas industries in the U.S.⁵⁷, about 35 percent of which is treated and discharged to surface water bodies. Some brines contain high concentrations of Ca²⁺, Mg²⁺, and Fe²⁺ ions. Table 1.1 shows the Mg²⁺ and Ca²⁺ ions concentrations in seawater and in various regional brine solutions.

Table 1.1 Mg²⁺ and Ca²⁺ ion concentrations (mg/L) in seawater and brines

Sources of reactive species	Mg ²⁺	Ca ²⁺	Reference
Oceanwater	1350	412	Wang(2010) ⁵⁸
Brine samples from Oriskany, Pennsylvania	2490	41000	Y.Soong(2006) ⁵⁹
Deep aquifer brine from Paradox Valley, Colorado ^a	1220	10900	Rosenbauer(2005) ⁶⁰
Brine samples from 1158 m well in Guernsey, Ohio	3440	19570	Druckenmiller(2005) ⁶¹
Brine samples from 1030 m well in Youngstown, Ohio	2055	19350	Druckenmiller(2005) ⁶¹

a : A synthetic solution to approximate the composition of deep brine from Paradox Valley

1.2.3.2 Previous studies on CO₂ mineralization using cations

The concept of CO₂ mineralization using reactive cations for sequestration was first proposed by Dunsmore in 1992⁶². He suggested that calcium/magnesium-rich brine from the subsurface could be used to sequester CO₂, forming calcium/magnesium carbonates. Later researchers also took on the issue. For example, Soong et al.⁶³ and Druckenmiller et al.⁶¹ conducted laboratory experiments on ex situ CO₂ mineralization using brine samples collected from different aquifers as a source of reactive cations, and potassium hydroxide (KOH) as a caustic material for correcting the pH of the brine at temperatures between 50-170 °C and at CO₂ pressures ranging from 0.34-7.63 MPa. The researchers confirmed that initial brine pH played a major role in the precipitation of carbonate minerals as opposed to temperature and pressure, which had less of an impact. Alkaline fly ash⁵⁹ and bauxite residue⁶⁴ were also used as a caustic

material to react with brine for CO₂ sequestration. The main carbonate minerals obtained in the above experiments were all calcite, indicating the main reactive cations involved were Ca²⁺ ions.

For CO₂ mineralization using Mg²⁺ ions, the only published work was conducted by Ferrini et al.⁶⁵ in 2009. In their experiments, compressed CO₂ reacted with magnesium chloride solution (~7 g/L of Mg²⁺) at room temperature (20 °C) and atmospheric CO₂ pressure, forming the mineral nesquehonite (Mg(OH)(HCO₃)•2H₂O). The pH range for the formation of nesquehonite was reported to be 7.8-8.2, controlled by the addition of aqueous ammonia. The reaction rate was relatively fast and 81.7% CO₂ was captured to form nesquehonite. It should be noted that the researchers did not investigate the effects of temperature and pH on the kinetics of nesquehonite formation.

Scientists at the California corporation, Calera^{66,67}, have also been studying CO₂ mineralization using cations with some interesting results. Calera's process is referred to as Mineralization via Aqueous Precipitation (MAP), in which CO₂ gas is absorbed into the water and reacts with alkaline metals (Mg²⁺, Ca²⁺) to form solid mineral carbonates or soluble bicarbonates. The solution pH controller is sodium hydroxide (NaOH) produced from an electrochemistry process referred to as the Alkalinity Based on Low Energy (ABLE) process, in which salt (NaCl) is split to form an alkaline solution and an acid using electricity. Although this process is currently demonstrated at two plants (in California and in Latrobe Valley in southeast Australia), Calera has released insufficient kinetic data to judge its efficacy.

1.2.3.3 Present study of CO₂ mineralization using reactive Mg²⁺ and/or Ca²⁺ ions

In the present work, gaseous CO₂ reacts with reactive Mg²⁺ and/or Ca²⁺ ions (with a focus on Mg²⁺) in an aqueous solution, capturing and converting CO₂ gas into environmentally benign and geologically stable carbonate in a solid form. Compared to other mineralization options, this process has two features:

- 1) Reactive species, such as Mg²⁺, Ca²⁺ cations, instead of natural rocks are used as raw materials, meaning that no costly extraction or pretreatment of minerals is needed.
- 2) This process is conducted at atmospheric CO₂ pressure and nearly ambient temperature (40 °C) while other options use high temperature (150—400 °C) and high CO₂ pressure (40—150 atm).

1.3 Thesis Outline

The main objective of this thesis is to study ex situ CO₂ mineralization for sequestration using reactive Mg²⁺ and/or Ca²⁺ ions at nearly ambient conditions. This study will emphasize the use of Mg²⁺ ions because magnesium carbonate has a higher weight proportion of CO₂ than calcium carbonate and seawater has much higher concentrations of Mg²⁺ than Ca²⁺ ions.

Chapter 1 introduces the topic of CO₂ sequestration and provides a literature review of the various approaches and processes that have been studied to date. Chapter 2 describes the thermodynamic properties and experimental results with respect to ex situ CO₂ mineralization using Mg²⁺ ions alone. The characterization of the solid product, nesquehonite (Mg(OH)(HCO₃)•2H₂O), is also provided. Chapter 3 studies the effects of stirring speed, aeration, additive sodium chloride (NaCl), ultrasonic, temperature and initial solution pH on the kinetics involved in the precipitation of nesquehonite. Chapter 4 presents the experimental investigations on using Ca²⁺ ion alone and using Mg²⁺ and Ca²⁺ ions together for CO₂ precipitation. Chapter 5 summarizes the work and provides suggestions for future work.

1.4 References

1. Dickinson, R.E. and R.J. Cicerone, *Future global warming from atmospheric trace gases*. 1986.
2. Cline, W.R., *The economics of global warming*. 1992: Peterson Institute.
3. Vitousek, P.M., *Beyond global warming: ecology and global change*. Ecology, 1994. **75**(7): p. 1861-1876.
4. Jacobson, M.Z., *Review of solutions to global warming, air pollution, and energy security*. Energy & Environmental Science, 2009. **2**(2): p. 148-173.
5. Pachauri, R.K., *Climate Change 2007: Synthesis Report. Contribution of Working Groups I, II and III to the Fourth Assessment Report of the Intergovernmental Panel on Climate Change*. Vol. 446. 2007: IPCC.
6. D'alessandro, D., B. Smit, and J.R. Long, *Carbon dioxide capture: prospects for new materials*. Angew. Chem., Int. Ed, 2010. **49**: p. 6058–6082.
7. *Inventory of U.S. Greenhouse Gas Emissions and Sinks: 1990-2009*.
8. Etheridge, D., et al., *Natural and anthropogenic changes in atmospheric CO₂ over the last 1000 years from air in Antarctic ice and firn*. Journal of Geophysical Research, 1996. **101**(D2): p. 4115-4128.
9. Keeling, C. and T. Whorf, *Atmospheric carbon dioxide record from Mauna Loa*. Trends: A Compendium of Data on Global Change. Carbon Dioxide Information Analysis Center, Oak Ridge National Laboratory, Oak Ridge, TN, 2008.

10. EIA, U., *International energy outlook*. Washington, DC, USA: United States Energy Information Administration, 2009.
11. Reichle, D., et al., *Carbon sequestration research and development*. Office of Science, Office of Fossil Energy, US Department of Energy, 1999.
12. Yang, H., et al., *Progress in carbon dioxide separation and capture: A review*. Journal of Environmental Sciences, 2008. **20**(1): p. 14-27.
13. Riahi, K., E.S. Rubin, and L. Schrattenholzer, *Prospects for carbon capture and sequestration technologies assuming their technological learning*. Energy, 2004. **29**(9): p. 1309-1318.
14. Drange, H. and P. Haugan, *Carbon dioxide sequestration in the ocean: The possibility of injection in shallow water*. Energy Conversion and Management, 1992. **33**(5-8): p. 697-704.
15. Scott, K.N., *Day after Tomorrow: Ocean CO₂ Sequestration and the Future of Climate Change*, The. Geo. Int'l Env'tl. L. Rev., 2005. **18**: p. 57.
16. Lackner, K.S., *Carbonate chemistry for sequestering fossil carbon*. Annual review of energy and the environment, 2002. **27**(1): p. 193-232.
17. Wisniewski, J., et al., *Carbon dioxide sequestration in terrestrial ecosystems*. 1993, Environmental Protection Agency, Corvallis, OR (United States). Environmental Research Lab.
18. Bradshaw, J. and P. Cook, *Geological sequestration of carbon dioxide*. Environmental Geosciences, 2001. **8**(3): p. 149.
19. Marini, L., *Geological sequestration of carbon dioxide: thermodynamics, kinetics, and reaction path modeling*. Vol. 11. 2007: Elsevier Science.
20. Holloway, S., *Underground sequestration of carbon dioxide—a viable greenhouse gas mitigation option*. Energy, 2005. **30**(11): p. 2318-2333.
21. Gillian, M., et al., *Development of integrated system for biomimetic CO₂ sequestration using the enzyme carbonic anhydrase*. Energy & fuels, 2001. **15**(2): p. 309-316.
22. Mirjafari, P., K. Asghari, and N. Mahinpey, *Investigating the application of enzyme carbonic anhydrase for CO₂ sequestration purposes*. Industrial & engineering chemistry research, 2007. **46**(3): p. 921-926.
23. Brown, L.M. and K.G. Zeiler, *Aquatic biomass and carbon dioxide trapping*. Energy Conversion and Management. **34**(9-11): p. 1005-1013.
24. Usui, N. and M. Ikenouchi, *The biological CO₂ fixation and utilization project by RITE(1) -- Highly-effective photobioreactor system*. Energy Conversion and Management, 1997. **38**(Supplement 1): p. S487-S492.
25. Skjånes, K., P. Lindblad, and J. Muller, *BioCO₂ — A multidisciplinary, biological approach using solar energy to capture CO₂ while producing H₂ and high value products*. Biomolecular Engineering, 2007. **24**(4): p. 405-413.
26. Chakraborty, A., G. Astarita, and K. Bischoff, *CO₂ absorption in aqueous solutions of hindered amines*. Chemical Engineering Science, 1986. **41**(4): p. 997-1003.
27. Rao, A.B. and E.S. Rubin, *A technical, economic, and environmental assessment of amine-based CO₂ capture technology for power plant greenhouse gas control*. Environmental science & technology, 2002. **36**(20): p. 4467-4475.
28. Rochelle, G.T., *Amine scrubbing for CO₂ capture*. Science, 2009. **325**(5948): p. 1652.

29. Rangwala, H., et al., *Absorption of CO₂ into aqueous tertiary amine/MEA solutions*. The Canadian Journal of Chemical Engineering, 1992. **70**(3): p. 482-490.
30. Lackner, K.S., *A guide to CO₂ sequestration*. Science, 2003. **300**(5626): p. 1677.
31. Holloway, S., *Storage of fossil fuel-derived carbon dioxide beneath the surface of the earth*. Annual review of energy and the environment, 2001. **26**(1): p. 145-166.
32. Korbøl, R. and A. Kaddour, *Sleipner vest CO₂ disposal-injection of removed CO₂ into the utsira formation*. Energy Conversion and Management, 1995. **36**(6): p. 509-512.
33. Lewicki, J., et al., *Surface CO₂ leakage during the first shallow subsurface CO₂ release experiment*. 2008.
34. Le Guern, F. and G.E. Sigvaldason, *The Lake Nyos Event, and Natural CO₂ Degassing, II*. 1990.
35. Tazieff, H., *Mechanisms of the Nyos carbon dioxide disaster and of so-called phreatic steam eruptions*. Journal of volcanology and geothermal research, 1989. **39**(2-3): p. 109-116.
36. Lockwood, J.P. and M. Rubin, *Origin and age of the Lake Nyos maar, Cameroon*. Journal of volcanology and geothermal research, 1989. **39**(2-3): p. 117-124.
37. Ide, S.T., S.J. Friedmann, and H.J. Herzog. *CO₂ leakage through existing wells: current technology and regulations*. 2006.
38. Zevenhoven, R., J. Fagerlund, and J.K. Songok, *CO₂ mineral sequestration: developments toward large-scale application*. Greenhouse Gases: Science and Technology, 2011. **1**(1): p. 48-57.
39. Coleman, R.G. and W.P. Irwin, *North American Ophiolites*. 1977: State of Oregon, Dept. of Geology and Mineral Industries.
40. Goff, F. and K. Lackner, *Carbon Dioxide Sequestering Using Ultramafic Rocks*. Environmental Geosciences, 1998. **5**(3): p. 89-102.
41. Lackner, K.S., et al., *Carbon dioxide disposal in carbonate minerals*. Energy, 1995. **20**(11): p. 1153-1170.
42. Herzog, H., *Carbon sequestration via mineral carbonation: overview and assessment*. Cambridge, Massachusetts: Massachusetts Institute of Technology, Laboratory for Energy and the Environment, 2002.
43. Huijgen, W., *Carbon dioxide sequestration by mineral carbonation*. Energy, 2003(February): p. 1-52.
44. Mazzotti, M., et al., *Mineral carbonation and industrial uses of carbon dioxide*. IPCC Special Report on Carbon dioxide Capture and Storage, 2005: p. 321-338.
45. Seifritz, W., *CO₂ disposal by means of silicates*. Nature, 1990. **345**.
46. Kojima, T., et al., *Absorption and fixation of carbon dioxide by rock weathering*. Energy Conversion and Management, 1997. **38**: p. S461-S466.
47. Robie, R.A. and B.S. Hemingway, *Thermodynamic properties of minerals and related substances at 298.15 K and 1 bar (10⁵ Pascals) pressure and at higher temperatures*. US Geol. Survey Bull., vol. 2131, p. 461-461 (1995). 1995. **2131**: p. 461-461.
48. Lackner, K.S., D.P. Butt, and C.H. Wendt, *Progress on binding CO₂ in mineral substrates*. Energy Conversion and Management, 1997. **38**: p. S259-S264.

49. Wendt, C., et al., *Thermodynamic Calculations for Acid Decomposition of Serpentine and Olivine in MgCl₂ Melts, III. Heat Consumption in Process Design*. 1998, Tech. Report No. LA-UR-98.
50. Nilson, D. and G. Hundley, *Preliminary feasibility study of the sequestration of carbon dioxide gas with minerals: a study of the LANL aqueous process*. Albany Research Center, US DoE, 1999.
51. Newall, P., et al., *CO₂ storage as carbonate minerals*. 1999: CSMA Consultants Ltd.
52. O'Connor, W.K., et al., *Carbon dioxide sequestration by direct mineral carbonation: results from recent studies and current status*. 2001, Albany Research Center (ARC), Albany, OR.
53. O'Connor, W., et al., *Carbon dioxide sequestration by ex-situ mineral carbonation*. 2000, Albany Research Center (ARC), Albany, OR.
54. O'Connor, W., et al. *Continuing studies on direct aqueous mineral carbonation for CO₂ sequestration*. 2002.
55. Gerdemann, S.J., et al., *Ex situ aqueous mineral carbonation*. Environmental science & technology, 2007. **41**(7): p. 2587-2593.
56. O'Connor, W., et al., *Aqueous mineral carbonation*. Final Report, DOE/ARC-TR-04, 2005. **2**.
57. Kharaka, Y., et al. *Can produced water be Reclaimed? Experience with placerita oil field, California*. 1998.
58. Wang, W., M. Hu, and C. Ma. *Possibility for CO₂ Sequestration Using Sea Water*: IEEE.
59. Soong, Y., et al., *CO₂ sequestration with brine solution and fly ashes*. Energy Conversion and Management, 2006. **47**(13): p. 1676-1685.
60. Rosenbauer, R.J., T. Koksalan, and J.L. Palandri, *Experimental investigation of CO₂-brine-rock interactions at elevated temperature and pressure: Implications for CO₂ sequestration in deep-saline aquifers*. Fuel processing technology, 2005. **86**(14-15): p. 1581-1597.
61. Druckenmiller, M.L. and M.M. Maroto-Valer, *Carbon sequestration using brine of adjusted pH to form mineral carbonates*. Fuel processing technology, 2005. **86**(14-15): p. 1599-1614.
62. Dunsmore, H., *A geological perspective on global warming and the possibility of carbon dioxide removal as calcium carbonate mineral*. Energy Conversion and Management, 1992. **33**(5-8): p. 565-572.
63. Soong, Y., et al., *Experimental and simulation studies on mineral trapping of CO₂ with brine*. Energy Conversion and Management, 2004. **45**(11): p. 1845-1859.
64. Dilmore, R., et al., *Sequestration of CO₂ in Mixtures of Bauxite Residue and Saline Wastewater*. Energy & fuels, 2007. **22**(1): p. 343-353.
65. Ferrini, V., C. De Vito, and S. Mignardi, *Synthesis of nesquehonite by reaction of gaseous CO₂ with Mg chloride solution: Its potential role in the sequestration of carbon dioxide*. Journal of Hazardous Materials, 2009. **168**(2-3): p. 832-837.
66. Constantz, B.R., et al., *METHODS OF SEQUESTERING CO₂*. 2008, US Patent App. 20,090/169,452.
67. Kolstad, C. and D. Young, *Cost Analysis of Carbon Capture and Storage for the Latrobe Valley*. University of California, Santa Barbara, 2010: p. 36.

Chapter 2

CO₂ Mineralization Using Reactive Mg²⁺ Ions

2.1 Introduction

This chapter details an alternative approach to the capture and storage of CO₂: the ex situ mineralization of CO₂ using reactive Mg²⁺ ions to capture and convert CO₂ gas into stable and safe solid carbonates before it enters the atmosphere. There are two reasons that we focus on Mg²⁺ ions rather than Ca²⁺ ions. First, fewer studies have addressed the possibility of using Mg²⁺ ions in this way. Second, in comparison to Ca²⁺ ions, Mg²⁺ ions have two important advantages: (i) there is a higher weight proportion of CO₂ in magnesium carbonates than in calcium carbonates due to the lower molecular weight of Mg, and (ii) seawater contains a much higher concentration of Mg²⁺ ions.

The approach discussed herein involves two steps. In Step 1, gaseous CO₂ is dissolved in MgCl₂ aqueous solution to form a soluble magnesium bicarbonate (Mg(HCO₃)₂) species. In Step 2, the soluble Mg(HCO₃)₂ decomposes and is transformed into a carbonate mineral in a solid form. Under ambient conditions, Step 1 proceeds rapidly, while Step 2 is very slow.

2.1.1 Nesquehonite

The solid carbonate obtained during Step 2 is a hydrated magnesium carbonate mineral called nesquehonite, which is a low-temperature carbonate typically formed in nature under near-surface conditions in coal mines, cave deposits, alkaline soils, serpentinite fractures, and as a weathering product of ultramafic rocks. Some investigators use the formula MgCO₃•3H₂O for nesquehonite, while others prefer Mg(OH)(HCO₃)•2H₂O. Recently, Frost, et al.¹ analyzed nesquehonite by a combination of infrared (IR) and infrared emission spectroscopy (IES), and showed the existence of OH⁻ and HCO₃⁻ units in the nesquehonite structure. As a result, the researchers suggested that the formula for nesquehonite ought to reflect the actual chemical reactions occurring during the precipitation step. Therefore, Mg(OH)(HCO₃)•2H₂O is the preferred chemical formula and will be used herein.

Nesquehonite is a monoclinic mineral, whose structure is characterized by infinite chains formed by corner-sharing MgO₆ octahedras, where one Mg ion is surrounded by 6 oxygen atoms^{2,3}. Within the chains, CO₃ groups link three MgO₆ octahedras by two common corners and

one edge, resulting in their strong deformation. Each Mg atom in the octahedra is coordinated by two H₂O ligands. One free H₂O molecule is located between the chains and hydrogen bonds interconnect these chains.

If nesquehonite is to be considered a viable solution for CO₂ storage, it is essential to have a thorough understanding of the mineral's structural stability. Ballirano et al.⁴ studied the thermal behaviour and structural stability of nesquehonite and found it to be stable up to 373 K, indicating that its storage capabilities would require little safety monitoring under typical temperature conditions at the Earth's surface. Specifically, the nesquehonite samples synthesized by Ferrini et al.⁵ were stored under ambient conditions and did not decompose within the three years of the study⁴. Moreover, additional thermal treatment will ultimately lead to the formation of magnesite, which is thermodynamically more stable (up to ~600K) than nesquehonite, making millions of years of CO₂ storage possible.

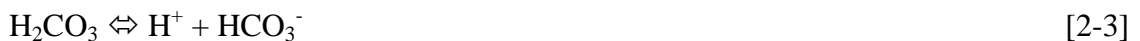
Although nesquehonite remains thermodynamically stable up to 373 K, it is not stable under acidic conditions, indicating that CO₂ could be released if nesquehonite is exposed to acid rain^{5,6}. Rain is normally slightly acidic (pH 5—7) due to the dissolution of atmospheric CO₂, sulfur and nitrogen oxides, and certain organic acids in water. However, due to human activities that produce more of these acidifying compounds, the pH of rain could be less than 4, resulting in the formation of sulfuric and nitric acid in rainwater. Teir et al.⁶ studied the stability of magnesium carbonate in nitric acid solutions of various acidities and found that no appreciable CO₂ release would occur in a solution of pH >2. In an earlier study, Brownlow⁷ reported that it would be unlikely for the pH of rain to be below 2; therefore, the risk of CO₂ release due to acid rain would be minimal. Teir et al.⁶ also studied the dissolution of magnesium carbonate under < 1 pH conditions and confirmed an insignificant release of CO₂.

In addition to its potential for CO₂ storage, nesquehonite has a number of industrial uses—for example, in construction as an aggregate substance in bricks, blocks, mortar, and other building materials. It can also contribute to the strength of eco-cement concretes due to the fact that its fibrous and needle-like crystal growths add micro-structural strength as a result of its 3D structures⁸. However, the application of nesquehonite at temperature above 373 K would be problematic due to the structural changes resulting in variations in mechanical strength.

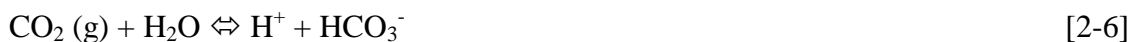
Many investigators have studied the laboratory synthesis of nesquehonite. Davis et al.⁹ and Ming et al.¹⁰ synthesized nesquehonite from saturated $\text{Mg}(\text{HCO}_3)_2$ solutions prepared by dissolving hydromagnesite ($\text{MgCO}_3 \cdot 4\text{Mg}(\text{OH})_2 \cdot 4\text{H}_2\text{O}$) in CO_2 -saturated water at room temperature. Other investigators have precipitated nesquehonite by mixing MgCl_2 and carbonate salt (e.g. Na_2CO_3 , $(\text{NH}_4)_2\text{CO}_3$) solutions¹¹⁻¹⁵. Ferrini et al.⁵ synthesized nesquehonite by injecting gaseous CO_2 into MgCl_2 solutions and adding ammonia solution (pH controller) into the solution. For the present work, the method of choice was similar to that used by Ferrini—with the modification that sodium hydroxide (NaOH) was used as a pH controller instead of an ammonia solution.

2.1.2 Chemical reaction

In Step 1, CO_2 gas is dissolved in water via the simplified Reactions [2-1] to [2-5], as shown below. Once the CO_2 gas is dissolved (Reaction [2-1]), carbonic acid forms (Reaction [2-2]). The latter then dissociates into bicarbonate (Reaction [2-3]) and carbonate ions (Reaction [2-5]). The dissolved CO_2 can also react with hydroxide ions (OH^-) to form bicarbonate ions (Reaction [2-4]). These reactions confirm that the pH of an aqueous solution decreases with the dissolution of CO_2 gas.

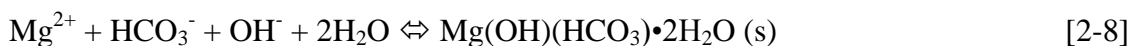


Combining Equations [2-1] — [2-5], the following equation is obtained,

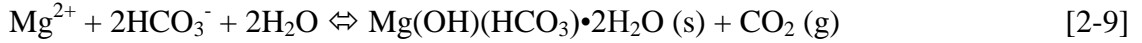


which is the overall reaction in Step 1 in the present work.

In Step 2, nesquehonite precipitates according to the following reactions:

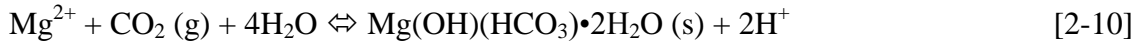


According to Reaction [2-7], the solution pH will increase and CO₂ gas will escape from the solution during nesquehonite precipitation. Combining Equations [2-7] and [2-8], the overall reaction for nesquehonite precipitation can be obtained, as shown in Equation [2-9].



Note that CO₂ gases dissolve in solution in Step 1, but then half of them flow away and the other half precipitate out from solution during nesquehonite precipitation (Step 2). Overall, the process equates to carbon sequestration with one Mg²⁺ ion capturing one CO₂ molecule, as shown in Reaction [2-10]. Also note that the dissolution of CO₂ gas in Step 1 is promoted by high CO₂ pressure and low temperature, and will lead to a decrease in solution pH. Conversely, the nesquehonite precipitation in Step 2 favors low CO₂ pressure and relatively high temperature (higher than ambient temperature but less than 50°C), resulting in an increase in solution pH. Therefore, the high temperature and high CO₂ pressure applied for the whole process is unlikely to facilitate carbon sequestration, which is partly why we chose near ambient conditions for the present study.

Combining Equations [2-6] and [2-9], the overall reaction for CO₂ mineralization is



As shown in Reaction [2-10], CO₂ mineralization will result in the undesirable acidization of the aqueous solution, which should be avoided. In the present work, therefore, NaOH was used to increase the solution pH while injecting CO₂ into the solution (Step 1).

2.1.3 Saturation index

The Mg-carbonate solubility equilibrium is very important in the water chemistry associated with CO₂ mineralization. To predict Mg-carbonate stability in water, saturation index (SI) is used to indicate whether the water will precipitate, dissolve, or remain in equilibrium with a particular Mg-carbonate. SI can be calculated via Equation [2-11] as shown below,

$$\text{SI} = \text{Log}(\text{IAP}/\text{K}) \quad [2-11]$$

where IAP is the ion activity product and K is the equilibrium constant.

For SI > 0, the mineral is supersaturated and tends to precipitate.

For $SI = 0$, the mineral is in equilibrium with water. The mineral is neither precipitated nor dissolved.

For $SI < 0$, the mineral is under-saturated and tends to dissolve in water.

2.2 Thermodynamic Calculation by *Visual Minteq*

Visual Minteq (VM) is a chemical equilibrium software used to calculate metal speciation, solubility equilibria, sorption, etc. since it can simulate the chemical composition of a solution in contact with gases and solid phases. In the present work, we utilized VM to construct species distribution diagrams and SI-pH diagram, as shown in Figures 2.1 to 2.4.

Three different carbonic species exist in a closed CO_2 - H_2O system: carbonic acid ($H_2CO_3(aq)$), bicarbonate ion (HCO_3^-) and carbonate ion (CO_3^{2-}). Figure 2.1 shows three corresponding pH ranges for the carbonic species that dominate in the CO_2 - H_2O system. Here, the concentration of $H_2CO_3(aq)$ species is assumed to be equal to the concentration of dissolved CO_2 . As shown, in a pH range of approximately 6–10 (the pH range used in this study was 6.6 – 7.5), the dominant species is HCO_3^- ion. Note that the total concentration of carbonic species was fixed at 1 M (Figure 2.1).

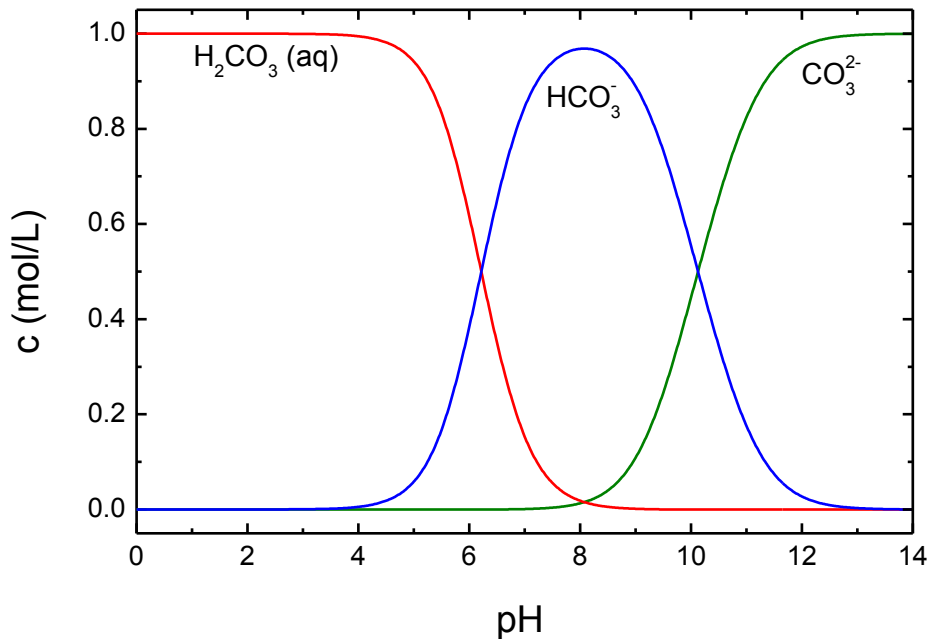


Figure 2.1 Carbonic species distribution in CO_2 - H_2O system at different pH levels at 22 °C

Regardless of the amount of CO_2 gas injected into an aqueous solution at atmospheric CO_2 pressure ($P_{\text{CO}_2} = 0.0038 \text{ atm}$), the pH of the solution will initially decrease due to the dissolution of CO_2 gas and then reach a minimum value and remain constant. For the present study, the minimum value is defined as equilibrium pH to distinguish it from the instant pH of the solution. The addition of OH^- ions into the solution can increase the equilibrium pH and the CO_2 gas solubility based on Reaction [2-4]. Figure 2.2 shows the concentrations of carbonic species at different equilibrium pH levels ranging from 6 – 10 at 22 °C. As shown, the dominant carbonic species is HCO_3^- ion, which confirms our initial results (Figure 2.1). Figure 2.2 also shows that both the HCO_3^- ion and total carbonic species increase with the equilibrium pH.

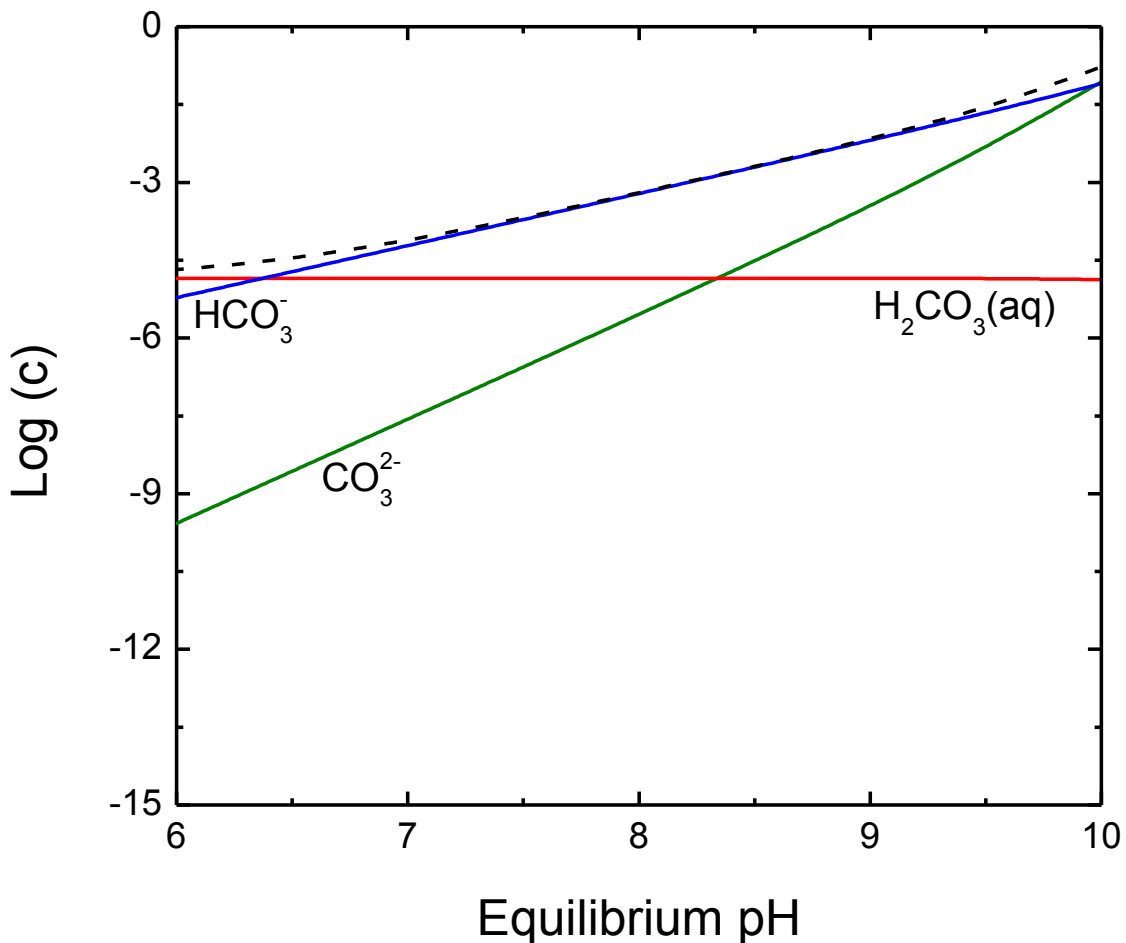


Figure 2.2 Carbonic species concentrations in CO_2 - H_2O system at different equilibrium pH levels at 22 °C based on infinite CO_2 gas at atmospheric CO_2 pressure. Dashed line represents the total concentration of carbonic species.

In the presence of reactive metal cations such as Mg^{2+} ions in the aqueous solution, carbonic species can react with these metal ions to form other species such as $\text{MgCO}_3(\text{aq})$, MgHCO_3^+ , etc. Figure 2.3 shows magnesium species concentrations at different pH levels ranging from 6 – 10, assuming 0.0583 M (~1400 mg/L) Mg^{2+} is introduced to the aqueous solution and an infinite amount of CO_2 gas at atmospheric CO_2 pressure is injected into the solution. As shown, the Mg^{2+} ion is the dominant Mg-species until the pH level reaches 9.6.

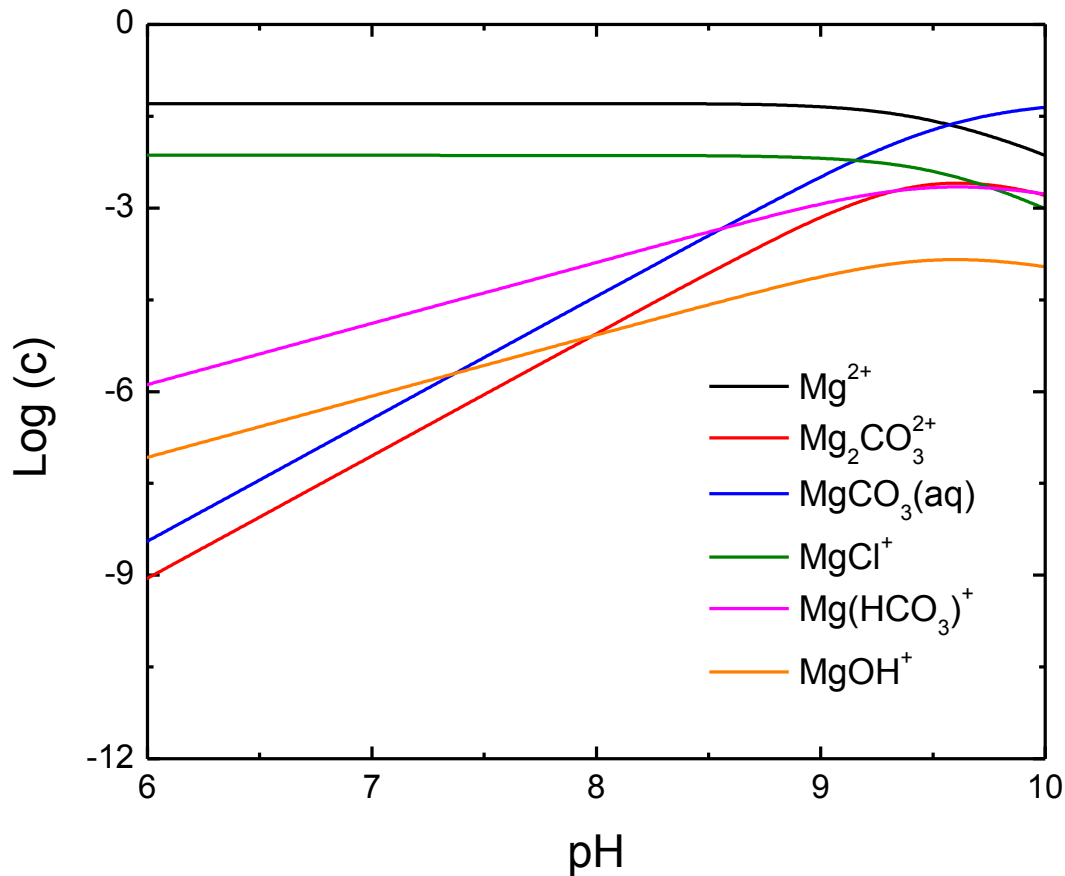


Figure 2.3 Mg-species concentrations in $\text{CO}_2\text{-Mg}^{2+}\text{-H}_2\text{O}$ system at different pH levels at 22 °C.

Figure 2.4 shows the SIs for a variety of Mg-carbonates in a $\text{Mg}^{2+}\text{-CO}_2\text{-H}_2\text{O}$ system in the pH range of 6 – 10 at 22 °C, given that 0.0583 M (~1400 mg/L) Mg^{2+} is introduced to the aqueous solution and an infinite amount CO_2 gas at atmospheric CO_2 pressure is injected into the

solution. As shown, when pH is lower than 8, all the Mg-carbonate minerals are under-saturated. When pH reaches 8, magnesite starts to precipitate from the solution. When pH increases further to 8.8, hydromagnesite and artinite start to precipitate. At pH levels at or above 9.5, lansfordite and nesquehonite begin to precipitate.

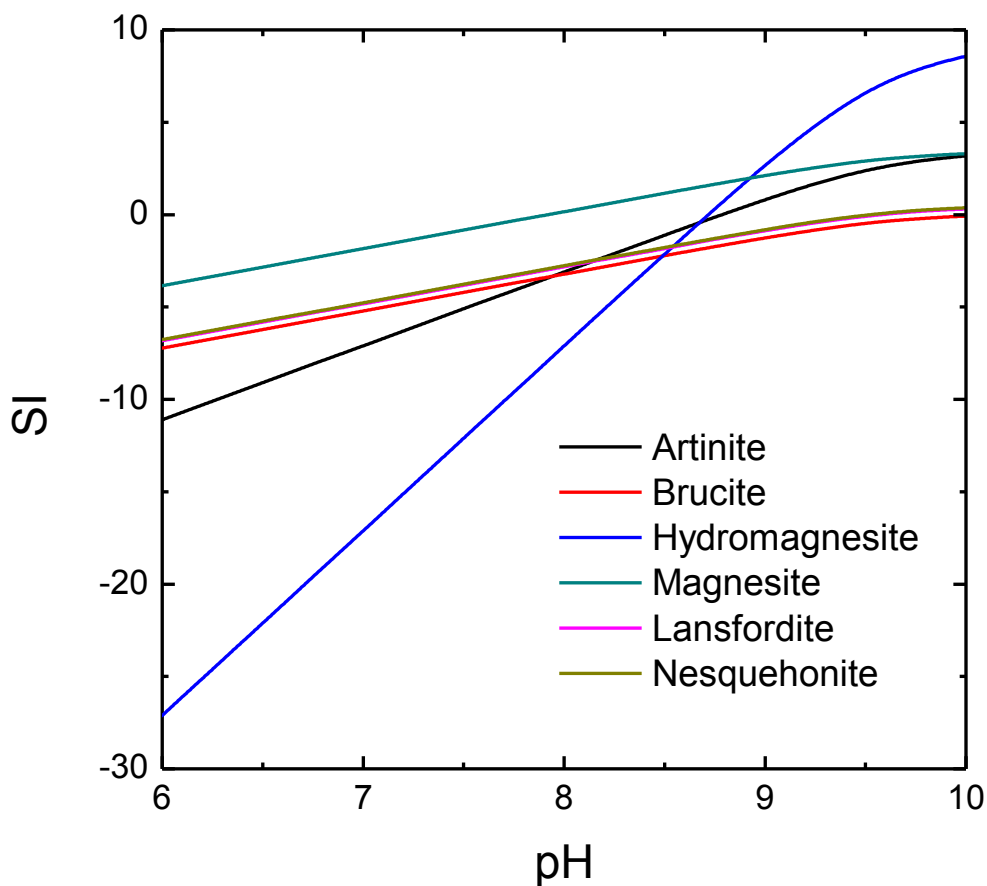


Figure 2.4 SI-pH diagram for different Mg-carbonate minerals at 22 °C.

2.3 Experiment

2.3.1 Materials

Anhydrous MgCl_2 (99%, Alfa Aesar) provided a source for magnesium, and compressed CO_2 gas (Bone Dry Grade, Airgas) and 10 N standardized NaOH solution as a pH controller

were used in our experiments. Dihydrated ethylenediaminetetraacetic acid disodium salt ($\text{Na}_2\text{H}_2\text{EDTA}\cdot 2\text{H}_2\text{O}$, 99+%, Alfa Aesar), pure Eriochrome Black T (EBT, indicator grade, Acros Organics), 2-methoxyethanol (ACS, 99.3+%, Alfa Aesar) and ammonia buffer solution pH 10 (Sigma-Aldrich) were used for standard EDTA titration. All experimental work for solution preparation, dilution, apparatus washing, etc. was done using the deionized Millipore water with a resistivity of 18.2 $\text{M}\Omega/\text{cm}$, which was obtained using a Direct-Q3 water purification system.

2.3.2 Procedure

Our study of the mineralization of CO_2 gas using reactive Mg^{2+} ions involved two steps; Figure 2.5 illustrates the schematics of the experimental set-up in these two steps. In Step 1, a stream of CO_2 gas was injected through a sparger into 700 mL of MgCl_2 solution in open air at room temperature ($\sim 22^\circ\text{C}$). The Mg^{2+} ion concentration used in the solution was 1400 mg/L, which corresponds to the average Mg^{2+} ion concentration in ocean water. As soon as the gas was injected, the solution pH decreased due to the dissolution of CO_2 gas in water. Diluted NaOH solutions were added dropwise into the solution using a syringe while injecting CO_2 gas in order to increase the pH until the equilibrium pH 6.9 was reached. Magnesium bicarbonate ($\text{Mg}(\text{HCO}_3)_2$) solution was formed in this step. In Step 2, the solution was brought to 40°C using a thermostat, and then agitated using a stirring blade at 640 rpm and aerated at 10 L/min. Under continuous stirring, a 4 mL sample was taken from the solution at each predetermined time interval in order to study the kinetics of the precipitation of nesquehonite. The samples were centrifuged, and then 1 mL of the supernatant solution was withdrawn using a pipette without disturbing the precipitate. The Mg^{2+} ion concentration ($[\text{Mg}^{2+}]$) in the supernate was measured using standard EDTA titration methods.

At the end of the precipitation experiment, the turbid solution was filtered, then washed with deionized water 3 times to remove any possible ionic remnants, and finally dried in an oven at 60°C for about 11 h. The dried samples were subjected to solid characterization.

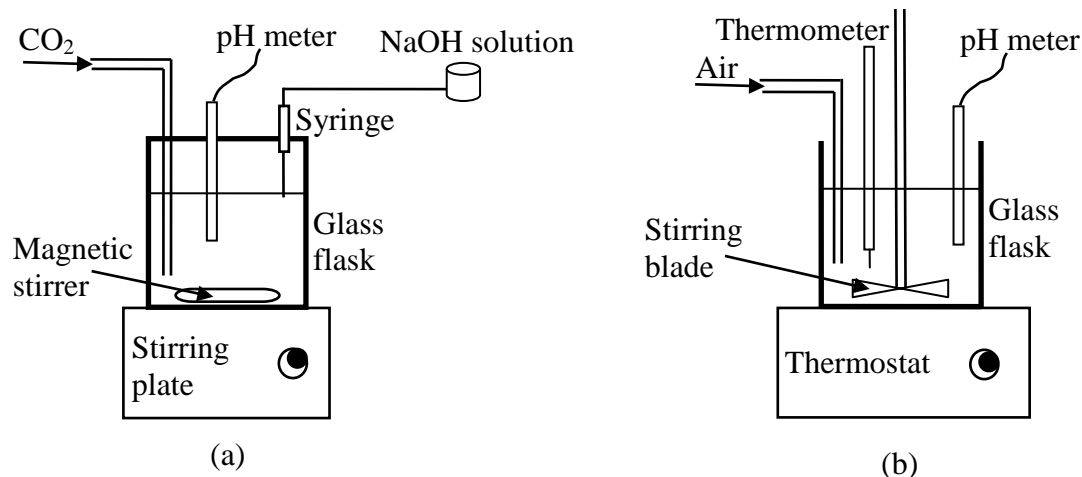


Figure 2.5 Schematics of the experimental set-up. (a): the set-up used in step 1; (b): the set-up used in step 2.

2.3.3 Standard EDTA titration

Ethylenediaminetetraacetic acid (EDTA), which is a weak acid, is widely used as a titrant to measure the concentration of Mg^{2+} or Ca^{2+} (or both) in an aqueous solution. It can react with metal ions to form coordination compounds (chelates). The reaction of Mg^{2+} with EDTA may be expressed as:



For the present study, 1 mL of the supernatant from each sample was pipetted into a 250 mL Erlenmeyer flask, and then 50 mL deionized water, 3 mL pH 10 buffer solution, and approximately 5 drops of EBT indicator were added to the flask. EBT reacts with Mg^{2+} ions and forms a chelate that is raspberry-red in color. The sample-solution in the flask was then swirled and titrated with standardized 0.005 M EDTA titrating solution. During titration, EDTA replaces the EBT and forms a more stable chelate with Mg^{2+} ions. When EBT is totally released by Mg^{2+} ions, it has a distinct blue color. Therefore, the endpoint of the titration was signaled by the color change from a raspberry-red to pure blue.

The molar Mg^{2+} ion concentration was calculated as follows:

$$c_{\text{Mg}^{2+}} = \frac{V_{\text{EDTA}} \cdot c_{\text{EDTA}}}{V_{\text{sample}}} \quad [2-13]$$

where V_{EDTA} is the volume of EDTA titrating solution used, c_{EDTA} is the molar concentration of standard EDTA titrating solution (0.005 M for the present work), and V_{sample} is the volume of the sample, which is 1 mL.

The EBT indicator solution was prepared by dissolving 0.5 g of EBT dye in 100 g of 2-methoxymethanol and stored in a light-resistant bottle.

2.3.4 Characterization of the solid product

The crystal structure and the morphology of the dried solid product were investigated using the X-ray powder diffraction (XRD) and field-emission scanning electron microscopy (FE-SEM, Zeiss, LEO 1550), respectively. X-ray energy dispersive spectrometer (EDS) analysis was also applied to determine the chemical composition of the solid product (with atomic numbers between boron and uranium).

2.4 Results

Figure 2.6 shows the changes of Mg^{2+} ion concentration ($[Mg^{2+}]$), percentage reduction of $[Mg^{2+}]$, and solution pH during nesquehonite precipitation (Step 2). The percent reduction of $[Mg^{2+}]$ is defined as the percentage of the Mg^{2+} ions that have been converted to nesquehonite, which can be calculated as follows:

$$\% \text{ Reduction of } [Mg^{2+}] = \frac{[Mg^{2+}]_i - [Mg^{2+}]_t}{[Mg^{2+}]_i} \times 100\% \quad [2-14]$$

where $[Mg^{2+}]_i$ refers to the Mg^{2+} ion concentration initially present in the solution, and $[Mg^{2+}]_t$ the Mg^{2+} ion concentration present in the solution at time t.

The efficiency of mineralization of CO_2 is equal to % reduction of $[Mg^{2+}]$.

As shown, the Mg^{2+} ion concentration decreased with time due to the precipitation of nesquehonite and reached its minimum at approximately 60 min. Accordingly, the % reduction of $[Mg^{2+}]$ increased with time and then reached its maximum. After 1h reaction time, only ~200 mg/L of Mg^{2+} ions remained in solution, representing a mineralization efficiency of 86%. As expected, the solution pH increased with time because of the increase in OH^- ion concentration due to Reaction [2-7] during nesquehonite precipitation.

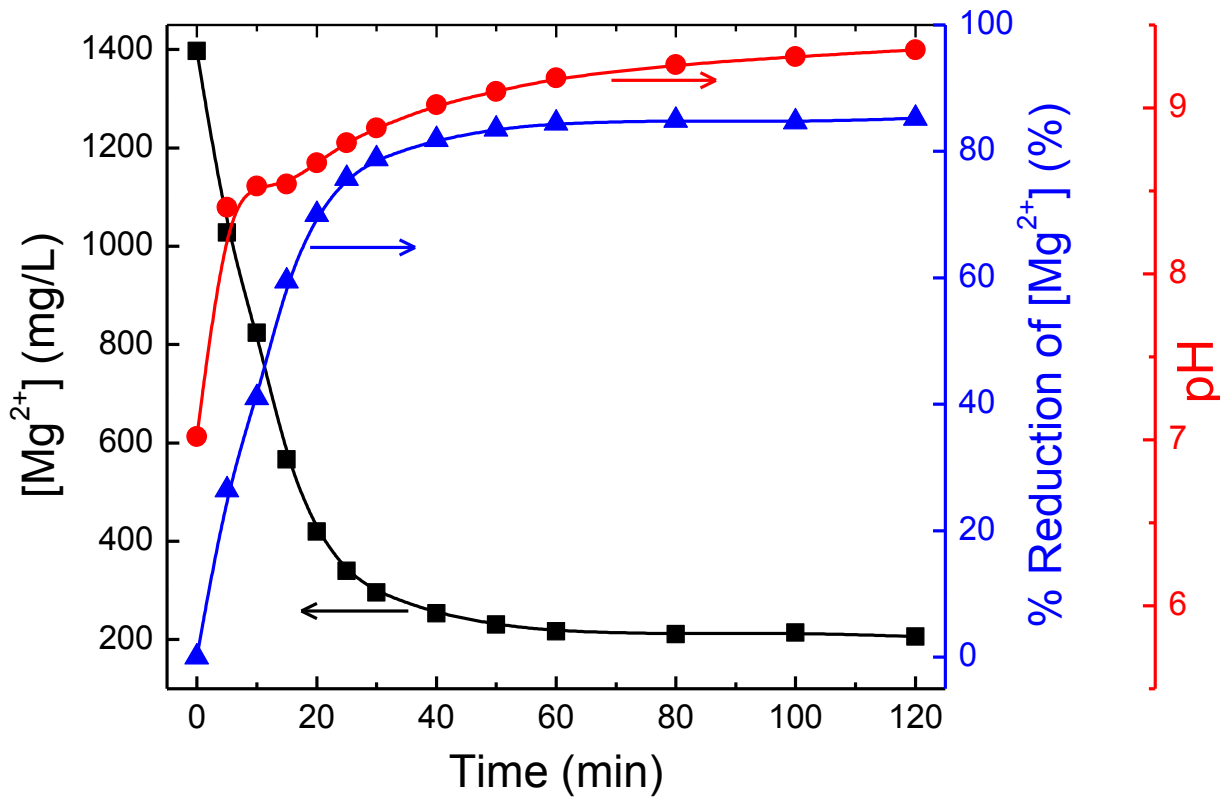


Figure 2.6 Changes in Mg²⁺ ion concentration ([Mg²⁺]), reduction of [Mg²⁺] and pH of the solution during nesquehonite formation.

Figure 2.7 shows the XRD pattern of the precipitated solid product obtained during CO₂ mineralization. Except for a few higher peaks in the reference data, very good agreement was found between the XRD pattern of our product and the nesquehonite pattern obtained from a database search, indicating the solid product to be nesquehonite. The narrow XRD peaks reflect the high degree of crystallinity of the precipitate obtained after 2 h of reaction.

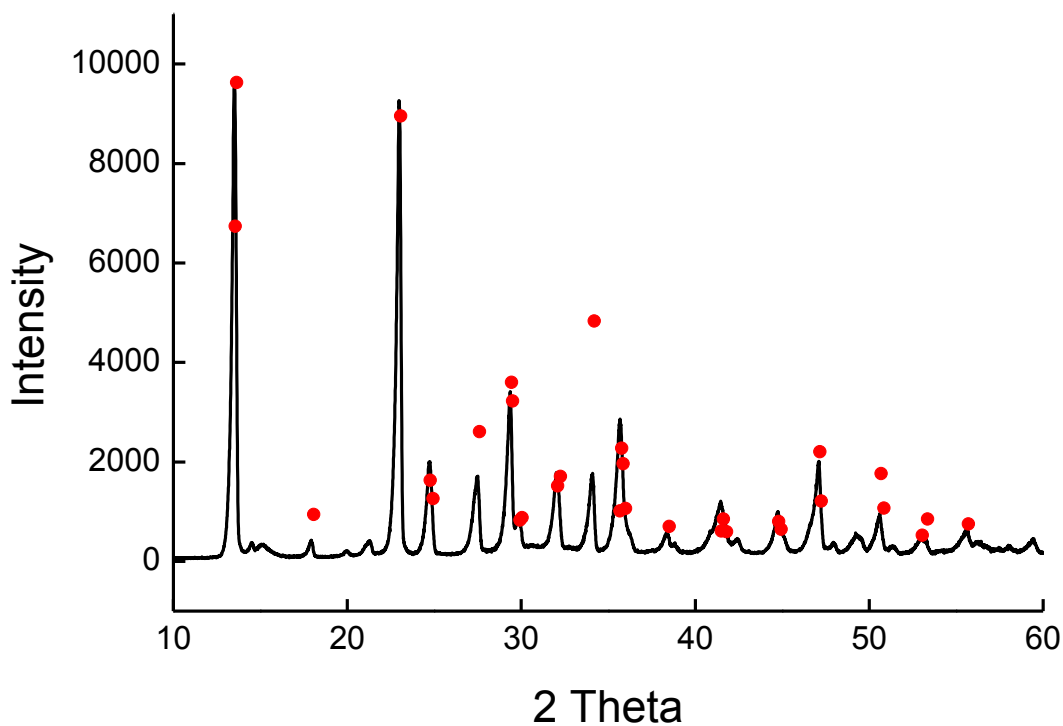


Figure 2.7 XRD pattern of the precipitated solid product compared with a reference XRD spectra of nesquehonite (red dots).

Figure 2.8 depicts SEM images of the solid product, which exhibit the typical morphology of nesquehonite crystals (well-formed needles). Subsequent EDS analysis also was in good agreement with Klopogge's¹¹ studies on the low temperature synthesis of nesquehonite, confirming the solid product to be nesquehonite (Figure 2.9).

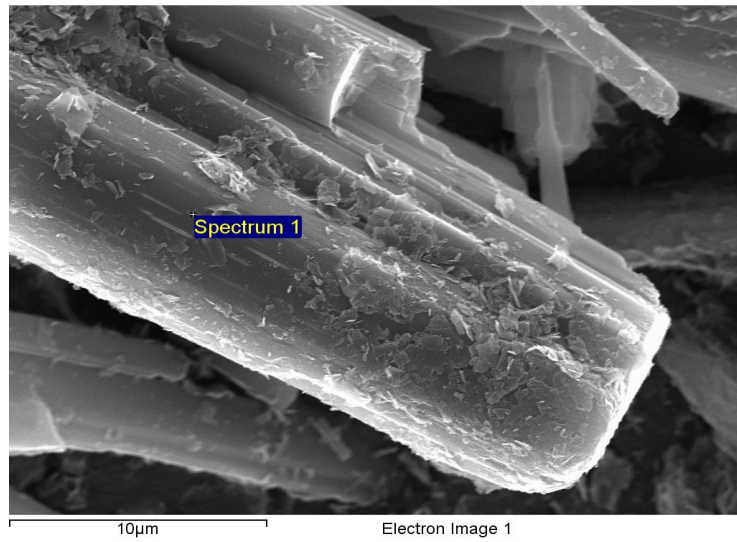
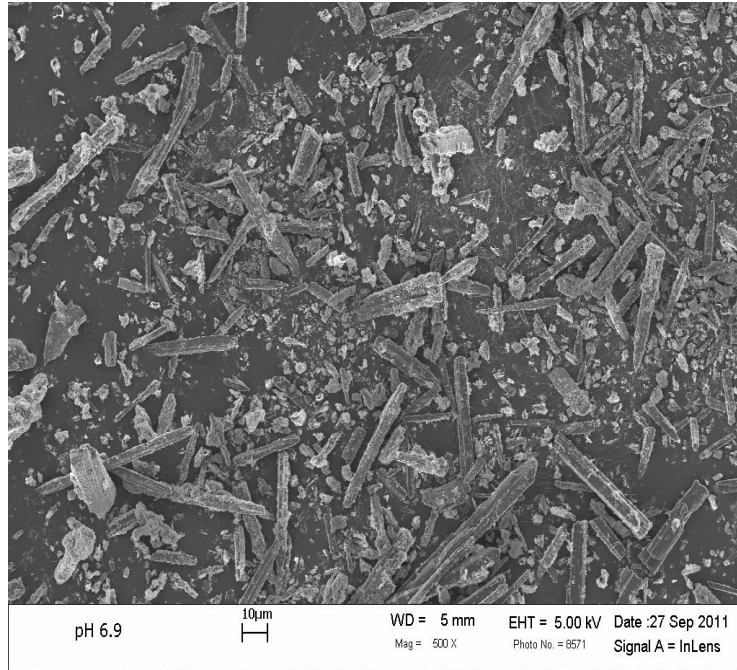


Figure 2.8 SEM images of the precipitated solid product.

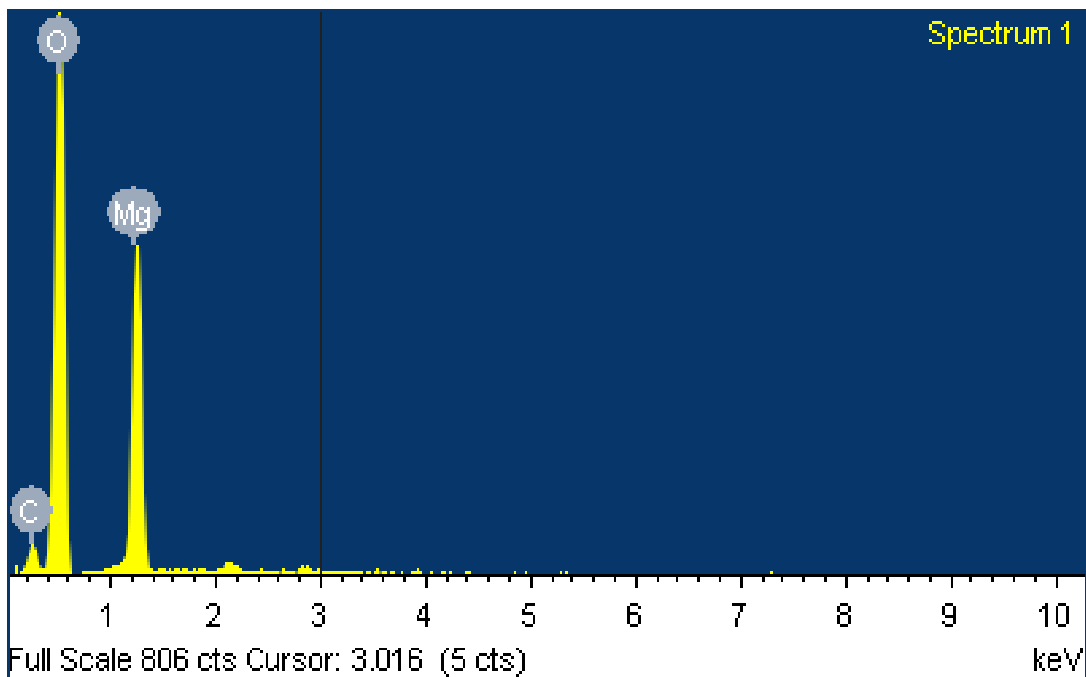


Figure 2.9 EDS analysis of the precipitated solid product.

Our experimental results showed that the solid product obtained in CO₂ mineralization process was nesquehonite. This did not match the thermodynamic calculation of the SI diagram conducted via VM, which indicates that under pH conditions of less than 9.5, the precipitation of magnesite will occur rather than nesquehonite. This outcome may be attributed to the fact that Visual Minteq only considers thermodynamic factors and does not incorporate kinetic factors. Numerous previous studies have confirmed that magnesite is the most stable magnesium carbonate regardless of temperature and CO₂ partial pressure^{16,17}. However, the formation of magnesite at ambient temperature is virtually impossible due to kinetic inhibitions. Typically, nesquehonite is the only mineral that can be precipitated from aqueous solution under ambient conditions, i.e., around 25 °C and atmospheric CO₂ partial pressure. In conclusion, our results agreed very well with previous studies on nesquehonite synthesis^{5,10-14}. At temperatures higher than 50 °C, hydromagnesite is usually formed by precipitation^{13,18}. At elevated temperatures and CO₂ partial pressure, magnesite can be formed directly¹². According to Christ and Hosteller¹⁶, nesquehonite and hydromagnesite could both transform to magnesite over time.

2.5 Discussion

2.5.1 Ocean capacity

Our results indicate that the approach discussed herein could achieve 86% efficiency when 1400 mg/L Mg^{2+} ions are used. Given that the total volume of seawater is estimated to be $1.5 \times 10^9 \text{ km}^3$, our experimental data indicate that a total of 3.4 million Giga tonnes (Gt) of CO_2 can be mineralized as nesquehonite using seawater with an average concentration of 1,400 mg/L Mg^{2+} ion. If Ca^{2+} cations are also used in CO_2 mineralization, 4.1 million Gt CO_2 could be sequestered. Using 2010 data, which indicates that 33.5 Gt CO_2 are released globally on an annual basis, available seawater could be used as a CO_2 sink for the next 122,000 years. Such a timespan should be considered “infinite”, given that humans began agriculture only about 10,000 years ago, and the earliest civilizations in Egypt, Greece, and China are perhaps 5,000 years old. Even if only 20% of the earth’s seawater were to be used for CO_2 mineralization, this would translate to about 24,400 years of CO_2 sequestration—in *theory* long enough to transition away from a fossil-fuel energy system to environmentally neutral alternatives.

Figure 2.10 shows the conceptual flowsheet of the process of CO_2 mineralization using $\text{Mg}^{2+}/\text{Ca}^{2+}$ ions in seawater. As shown, near an ocean, a mineralization plant could be built, where ocean water containing high level of $\text{Mg}^{2+}/\text{Ca}^{2+}$ ions and CO_2 gas from power plants are transported to and react with each other. Natural minerals such as limestone and olivine could be used to control the solution pH. The solid products obtained in this process such as nesquehonite could be marketed and used for industrial purposes.

Our findings are consistent with the general notion that the ocean could represent the largest sink for CO_2 capture. This notion is based on simple calculations of CO_2 solubility in seawater, which decreases with increasing temperature. If some of the Mg^{2+} ions dissolved in seawater are mineralized by CO_2 (as reported herein), this means that the seawater can literally serve as an infinitely large sink for CO_2 gas. It is possible that the geology controlled the atmospheric CO_2 concentration in the same manner over the eons.

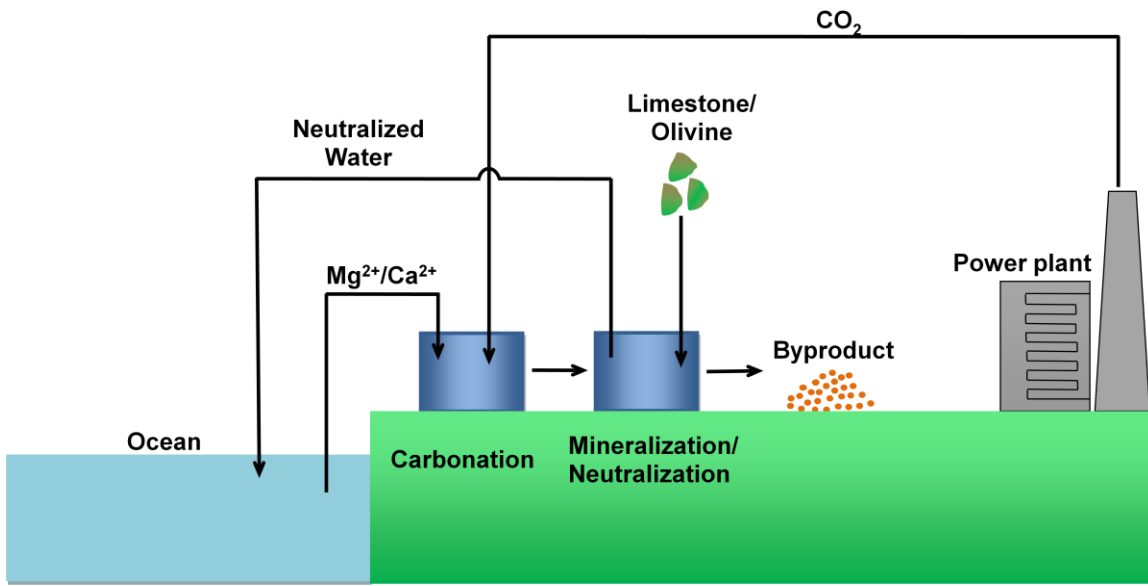


Figure 2.10 Conceptual flowsheet of the process of CO₂ mineralization using reactive Mg²⁺/Ca²⁺ ions.

2.5.2 Other magnesium sources

As discussed previously, saline brines produced as a byproduct of the oil and gas industries (so-called “produced water”), and rejected brines from the desalination process, could also provide a massive supply of magnesium. Currently, approximately 70 billion barrels of produced water are generated globally every year¹⁹, of which the U.S. contributes 20 to 30 billion barrels²⁰. About 65% of this water is re-injected into reservoirs to enhance oil recovery, while the remaining water is treated and discharged into surface water bodies—which is a costly process. The amount and composition of produced water varies according to geological formations, extraction methods and chemical treatment. On average, produced water is comprised of about 6% magnesium chloride²¹. Therefore, utilizing produced water in CO₂ mineralization processes can provide important magnesium sources, as well as result in increased water purity. The current experimental work employed magnesium chloride in concentrations much lower than produced water, suggesting that using produced water would result in faster kinetics during CO₂ mineralization.

2.5.3 Controlling pH

Both the dissolution of CO₂ gas into water and the conversion of bicarbonates into carbonates proceed more rapidly at relatively high pH levels. Avoiding acidization of the

aqueous solution is very important for successful CO₂ mineralization. For the current study, NaOH was used as an alkalinity source to maintain the solution pH. It should be noted, however, that while it was acceptable to use NaOH to study the chemical viability and potential of the new approach, the large-scale industrial application of this approach would be prohibitively expensive. Discussed below are some cheap methods possible for controlling the solution pH in the process of CO₂ mineralization.

Natural alkaline minerals such as limestone, olivine and serpentine could potentially be used to prevent the solution pH from becoming acidic in the presence of dissolved CO₂ based on the minimum solubility theory. Provided that a sufficient amount of pulverized limestone or forsterite was present in the aqueous solution, after CO₂ gas was injected into the solution, the dissolution of the mineral would consume the protons (H⁺) in the solution generated by the dissolution of CO₂ gas. Thus, the solution pH would increase, causing the equilibrium pH to be the same as the pH of minimum solubility. In effect, the alkaline minerals would act as a buffer.

Figure 2.11 depicts the solubility diagram for limestone at 25 °C and atmospheric CO₂ partial pressure. It was constructed using the thermodynamic data reported by Somasundaran and Agar²². As shown, limestone has a minimum solubility of pH 8.1, indicating that the mineral should act as a pH 8.1 buffer. Figure 2.12 shows the change in solution pH in the presence of limestone in the solution with and without injecting CO₂. As shown, in the presence of limestone in the solution, when CO₂ was injected into the solution, the solution pH rapidly decreased to around 6; when CO₂ injection was stopped, the pH increased toward the pH of minimum solubility of limestone.

Figure 2.13 depicts the solubility diagrams for forsterite at 25 °C and atmospheric CO₂ partial pressure. It was constructed using thermodynamic data from the computer program VM. As shown, the mineral has a minimum solubility at around pH 9, indicating that the mineral should act as a pH 9 buffer. The validity of the solubility diagram constructed in the present work may be given by the fact that the isoelectric point (IEP) of unweathered forsterite is pH 8.9 reported by Parks²³. Figure 2.14 shows the change in solution pH in the presence of olivine in the solution with and without injecting CO₂. As shown, in the presence of olivine in the solution, when CO₂ was injected into the solution, solution pH decreased to around 5; when CO₂ injection was stopped, the pH increased toward the pH of minimum solubility of olivine.

Figure 2.12 and 2.14 confirmed the possibility of using alkaline minerals to increase the solution pH, and thus to be used as a pH controller in the process of CO₂ mineralization. Natural minerals are much cheaper than NaOH and are abundant in nature, making the widespread commercial CO₂ mineralization more viable. Nonetheless, it took hours for the limestone and olivine to dissolve and raise the solution pH under ambient conditions. Methods to improve the kinetics of mineral dissolution should be further investigated in future work if alkaline minerals are to be applied in the process of CO₂ mineralization.

Other potential alkaline sources could be industrial wastes, such as slags from steel production, fly ashes from coal combustion, bauxite residues from the extraction of aluminum, and so forth. There are several advantages of using industrial wastes in this way: (i) Industrial wastes tend to be cheap, which reduces the costs associated with CO₂ mineralization. (ii) Industrial wastes are typically produced near sites with significant sources of CO₂ emission, which means that no transportation would be needed and the consumption of raw materials could be avoided. (iii) The reaction of industrial wastes with CO₂ tends to proceed rapidly due to the chemical instability of the former, which might reduce the energy costs of CO₂ mineralization. (iv) CO₂ sequestration using industrial waste could solve many environmental problems associated with cleaning and disposing them. Three examples of industrial wastes are provided below.

Steel manufacturing, one of the great CO₂ emitters, generates ~350 millions of tons of steel and iron slags annually all over the world²⁴. Steel slags consist of many compounds—but principally calcium, iron, silicon, aluminum, magnesium, and manganese oxides²⁵. Before it is treated, steel slag contains three major calcium phases (portlandite (Ca(OH)₂, Ca-(Fe)-silicate, and Ca-Fe-O), as well as other mineral phases including Mg-Fe-O, Fe-O, and also trace amounts of calcite (CaCO₃)^{26,27}. Its high oxide content renders steel slag highly alkaline (pH ~12), making it a good source of alkalinity for CO₂ mineralization.

Coal-burning power plants currently produce 600 million tons of fly ashes every year, with the U.S. responsible for about 110 million tons^{28,29}. More fly ashes will be produced in the near future due to increases in coal combustion to satisfy increasing industrial and domestic demands. Presently, only around 30% of the fly ashes are recycled or used as construction materials²⁸, while the remainder is disposed of in landfills or slurry ponds. Some Class-C fly

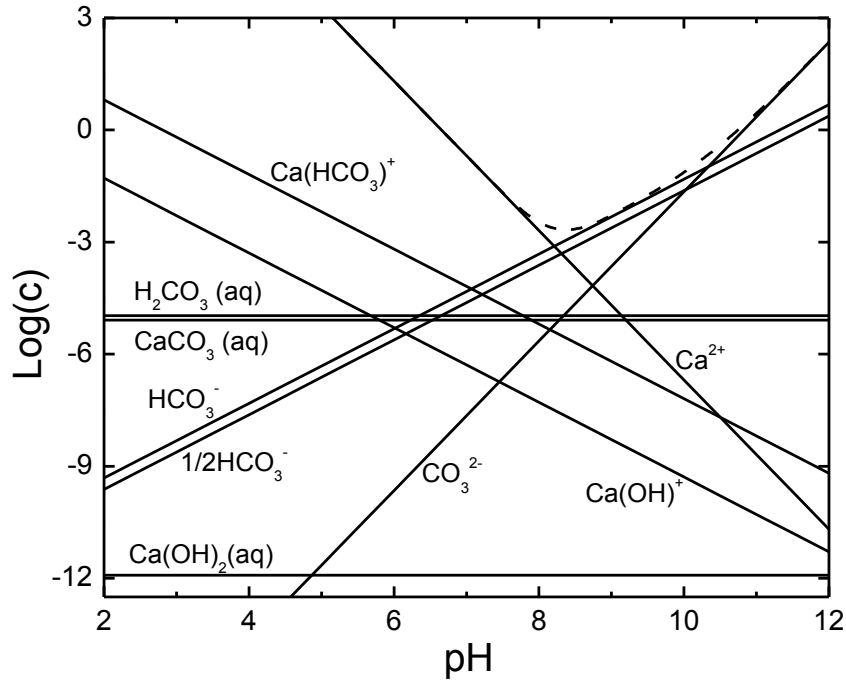


Figure 2.11 Solubility diagram of limestone at 25 °C and atmospheric CO_2 partial pressure. The dashed line represents the concentration of total dissolved species.

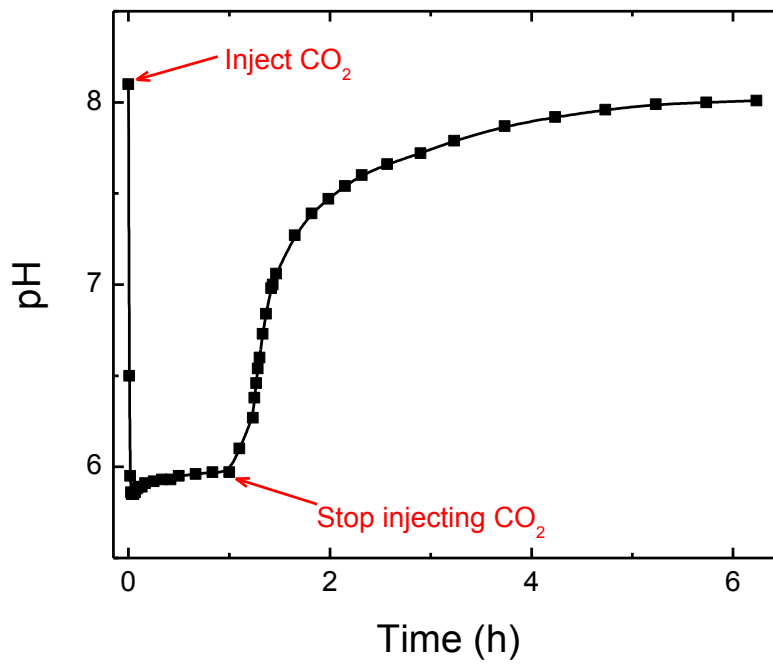


Figure 2.12 Changes in the solution pH in the presence of limestone with and without injecting CO_2 at 25 °C.

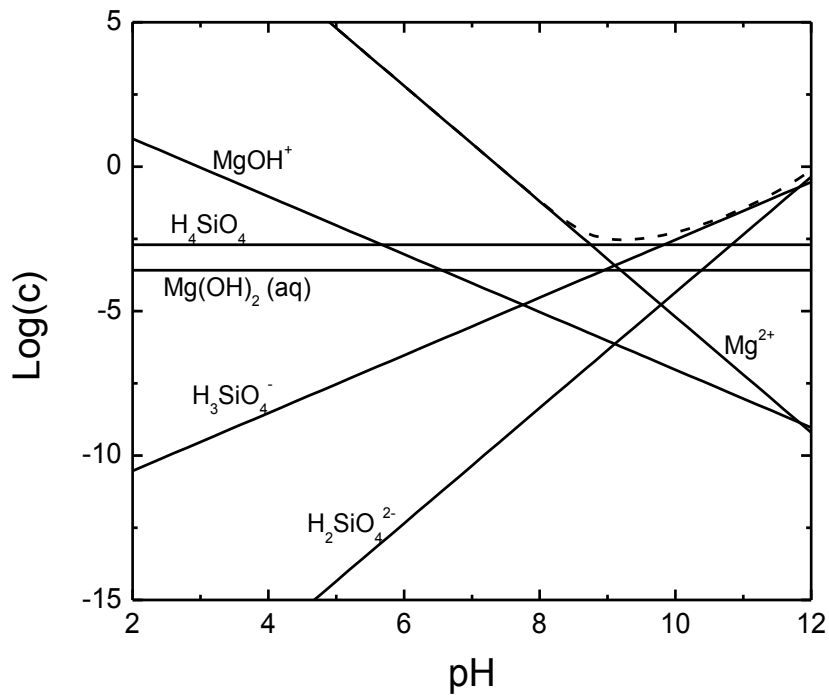


Figure 2.13 Solubility diagram of forsterite at 25 °C and atmospheric CO₂ partial pressure. The dashed line represents the concentration of total dissolved species.

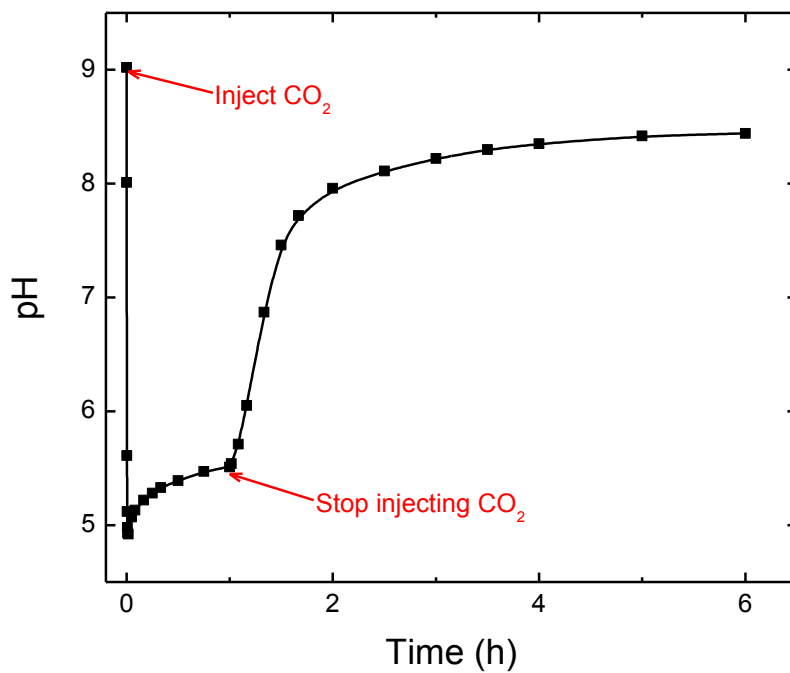


Figure 2.14 Changes in the solution pH in the presence of olivine with and without injecting CO₂ at 25 °C.

ashes feature high concentrations of basic calcium/magnesium oxides (CaO/MgO) and thus are highly alkaline. Therefore, fly ashes could be used to increase the solution pH during CO₂ mineralization. An added benefit is that fly ashes contain calcium/magnesium that could react with CO₂ to form carbonates, thereby improving the efficiency of CO₂ mineralization.

In the aluminum industry, over 70 million dry metric tons of bauxite residues are produced worldwide every year; additionally, there are currently in excess of 200 million tons of bauxite residue now stored in tailing ponds³⁰. The composition of this bauxite residue varies greatly depending on the composition of the bauxite ore and on processing parameters. Typically, bauxite residues consist of iron and titanium oxides, silica, calcium carbonates and unrecoverable alumina and caustic soda, rendering the bauxite residue highly alkaline (pH ~13 or higher). Also important to this discussion is that bauxite residue can create long-term environmental damage due to the leakage of alkaline liquid from impoundments into groundwater. Thus, future work should investigate the use of bauxite residues in CO₂ mineralization processes, which could not only help sequester CO₂, but also mitigate negative environmental impacts.

2.5.4 Advantages of the new approach

There are several advantages associated with the CO₂ mineralization processes discussed herein. First, compared to geological sequestration, this approach is suitable for safe and long-term storage of CO₂ because the solid product, nesquehonite, is thermodynamically and chemically stable. Second, compared to other mineralization methods using natural alkaline minerals (e.g., olivine and serpentine), this approach does not require energy-intensive extraction or mineral-activation processes because reactive Mg²⁺ ions are used. Plus, this approach can be carried out under nearly ambient conditions instead of at high temperatures (150–400 °C) and high CO₂ pressures (40 – 150atm), resulting in substantial energy savings and processing efficiency. Third, the process is kinetically favored and simple. Fourth, the resulting solid product, nesquehonite, could potentially be used in construction. Finally, the starting reactants are locally abundant; moreover, several types of industrial wastes that are produced near significant industrial sources of CO₂ emissions (e.g., steel works, cement production facilities, coal-burning energy plants) could be used, which would address important environmental concerns.

Although the geological sequestration of CO₂ is currently the method of choice due to its large-scale commercial application, it poses significant risks for CO₂ leakage and heavy metal leaching. In addition, this method is not always feasible due to locational restrictions. Therefore, CO₂ mineralization using reactive Mg²⁺ ions presents an excellent and promising alternative for CO₂ sequestration. In fact, this approach is highly favored where magnesium sources are significant or where considerable levels of CO₂ emissions and alkaline industrial wastes are both produced. With additional research and feasibility studies, CO₂ mineralization using reactive Mg²⁺ cations could be developed into a cost-effective, environmentally attractive process.

2.6 Conclusions

The present study discusses a potentially viable alternative to current methods for CO₂ sequestration, namely, CO₂ mineralization using reactive Mg²⁺ ions under nearly ambient conditions. Our experimental results confirmed that it is a kinetically-favorable process, as well as a procedure that could be conducted successfully at near ambient temperatures. Our results achieved up to 86% efficiency at 40 °C by stirring and aerating the solution for 1 h. This study also indicated that the *Visual Minteq* computer program is inadequate for predicting precipitation results in the Mg²⁺-CO₂-H₂O system. Additionally, our characterization of the solid products confirmed that nesquehonite was obtained. We also analyzed the capacity of seawater for CO₂ mineralization, and expanded the discussion of using magnesium and alkalinity sources with this approach. Finally, we demonstrated the significant potential of CO₂ mineralization using reactive Mg²⁺ ions for the sequestration of CO₂ gas.

2.7 References

1. Frost, R.L. and S.J. Palmer, *Infrared and infrared emission spectroscopy of nesquehonite Mg(OH)(HCO₃)·2H₂O-implications for the formula of nesquehonite*. Spectrochimica Acta Part A: Molecular and Biomolecular Spectroscopy, 2010.
2. Stephan, G.W. and C.H. MacGillavry, *The crystal structure of nesquehonite, MgCO₃·3H₂O*. Acta Crystallographica Section B, 1972. **28**(4): p. 1031-1033.
3. Giester, G., C.L. Lengauer, and B. Rieck, *The crystal structure of nesquehonite, MgCO₃·3H₂O, from Lavrion, Greece*. Mineralogy and Petrology, 2000. **70**(3): p. 153-163.
4. Ballirano, P., et al., *The thermal behaviour and structural stability of nesquehonite, MgCO₃·3H₂O, evaluated by in situ laboratory parallel-beam X-ray powder diffraction: New constraints on CO₂ sequestration within minerals*. Journal of Hazardous Materials, 2010. **178**(1-3): p. 522-528.

5. Ferrini, V., C. De Vito, and S. Mignardi, *Synthesis of nesquehonite by reaction of gaseous CO₂ with Mg chloride solution: Its potential role in the sequestration of carbon dioxide*. Journal of Hazardous Materials, 2009. **168**(2-3): p. 832-837.
6. Teir, S., et al., *Stability of calcium carbonate and magnesium carbonate in rainwater and nitric acid solutions*. Energy Conversion and Management, 2006. **47**(18): p. 3059-3068.
7. Brownlow, A.H., *Geochemistry, 2nd ed.* 1996: Prentice-Hall, New Jersey.
8. Harrison, A.J.W. and B.S.B.E. FCPA, *Tececo eco-cement masonry product update*.
9. Davies, P.J. and B. Bubela, *The transformation of nesquehonite into hydromagnesite*. Chemical Geology, 1973. **12**(4): p. 289-300.
10. Ming, D.W. and W.T. Franklin, *Synthesis and Characterization of Lansfordite and Nesquehonite*. Soil Sci. Soc. Am. J. **49**(5): p. 1303-1308.
11. Kloprogge, J.T., et al., *Low temperature synthesis and characterization of nesquehonite*. Journal of Materials Science Letters, 2003. **22**(11): p. 825-829.
12. Hänchen, M., et al., *Precipitation in the Mg-carbonate system--effects of temperature and CO₂ pressure*. Chemical Engineering Science, 2008. **63**(4): p. 1012-1028.
13. Cheng, W., Z. Li, and G.P. Demopoulos, *Effects of Temperature on the Preparation of Magnesium Carbonate Hydrates by Reaction of MgCl₂ with Na₂CO₃*. Chinese Journal of Chemical Engineering, 2009. **17**(4): p. 661-666.
14. Cheng, W. and Z. Li, *Nucleation kinetics of nesquehonite (MgCO₃·3H₂O) in the MgCl₂-Na₂CO₃ system*. Journal of Crystal Growth, 2010. **312**(9): p. 1563-1571.
15. Wang, Y., Z. Li, and G.P. Demopoulos, *Controlled precipitation of nesquehonite (MgCO₃·3H₂O) by the reaction of MgCl₂ with (NH₄)₂CO₃*. Journal of Crystal Growth, 2008. **310**(6): p. 1220-1227.
16. Christ, C. and P. Hostetler, *Studies in the system MgO-SiO₂-CO₂-H₂O (II); the activity-product constant of magnesite*. American Journal of Science, 1970. **268**(5): p. 439-453.
17. Kittrick, J. and F. Peryea, *Determination of the Gibbs free energy of formation of magnesite by solubility methods*. Soil Science Society of America Journal, 1986. **50**(1): p. 243-247.
18. Zhao, Y. and G. Zhu, *Thermal decomposition kinetics and mechanism of magnesium bicarbonate aqueous solution*. Hydrometallurgy, 2007. **89**(3-4): p. 217-223.
19. Veil, J. and M. Puder, *Regulatory considerations in the management of produced water—A US perspective*. Produced Water Management-Gas TIPS, 2005: p. 25-28.
20. Kharaka, Y., et al. *Can produced water be Reclaimed? Experience with placerita oil field, California*. 1998.
21. Kanagy, L.E., et al., *Design and performance of a pilot-scale constructed wetland treatment system for natural gas storage produced water*. Bioresource technology, 2008. **99**(6): p. 1877-1885.

22. Somasundaran, P. and G. Agar, *The zero point of charge of calcite*. Journal of colloid and Interface Science, 1967. **24**(4): p. 433-440.
23. Parks George, A., *Aqueous Surface Chemistry of Oxides and Complex Oxide Minerals*, in *Equilibrium Concepts in Natural Water Systems*. 1967, AMERICAN CHEMICAL SOCIETY. p. 121-160.
24. Miklos, P., *The utilization of electric arc furnace slags in Denmark*. Euroslag. *Engineering of slags. A scientific and technological challenge*. Proceedings of the 2nd European Slag ConferenceDüsseldorf, 2000.
25. Bonenfant, D., et al., *CO₂ sequestration potential of steel slags at ambient pressure and temperature*. Industrial & engineering chemistry research, 2008. **47**(20): p. 7610-7616.
26. Huijgen, W.J.J., G.J. Witkamp, and R.N.J. Comans, *Mineral CO₂ sequestration by steel slag carbonation*. Environmental science & technology, 2005. **39**(24): p. 9676-9682.
27. Huijgen, W.J.J. and R.N.J. Comans, *Carbonation of steel slag for CO₂ sequestration: leaching of products and reaction mechanisms*. Environmental science & technology, 2006. **40**(8): p. 2790-2796.
28. Montes-Hernandez, G., et al., *Mineral sequestration of CO₂ by aqueous carbonation of coal combustion fly-ash*. Journal of Hazardous Materials, 2009. **161**(2-3): p. 1347-1354.
29. Rostami, H. and W. Brendley, *Alkali ash material: a novel fly ash-based cement*. Environmental science & technology, 2003. **37**(15): p. 3454-3457.
30. Anich, I., et al. *The alumina technology roadmap*. 2002: TMS.

Chapter 3

A Kinetic Study of Nesquehonite Precipitation

3.1 Introduction

The second step in the process of CO₂ mineralization using reactive Mg²⁺ ions, as detailed in Chapter 2, is the conversion of soluble magnesium bicarbonate (Mg(HCO₃)₂) into the solid mineral nesquehonite (Mg(OH)(HCO₃)·2H₂O), which is kinetically a much slower process than CO₂ gas dissolution (Step 1). Therefore, it is important to improve the kinetics of nesquehonite precipitation.

Many investigators have studied the precipitation of nesquehonite from aqueous solutions under different experimental conditions¹⁻⁸. What they found was that temperature played an important role in the kinetics of the precipitation, as well as in the resulting products obtained from the aqueous Mg²⁺-CO₂-H₂O system. At low temperatures (0–45 °C), only the mineral nesquehonite can be precipitated from aqueous solution. Cheng et al.⁶ investigated the temperature effect on the nucleation kinetics of nesquehonite in an MgCl₂ – Na₂CO₃ system and concluded that temperature could strongly accelerate nesquehonite nucleation by decreasing the induction time period. At higher temperatures (> ~ 50 °C), basic magnesium carbonates are usually precipitated. In the present study, nesquehonite was selected as the target precipitate because of its low temperature preference and good filtration properties. Therefore, the temperature applied in the present work was within the temperature range of nesquehonite formation (0–45 °C).

In addition to temperature, the solution pH level is also believed to have a significant influence on the formation of carbonate minerals⁸⁻¹⁰. However, in the case of nesquehonite, there is currently no published data on the pH effects on the precipitation of this mineral.

In this study, therefore, the effects of reaction temperature and initial solution pH on the kinetics of nesquehonite precipitation from aqueous Mg(HCO₃)₂ solution were investigated. Other factors were also examined, including stirring speed, aeration, additive NaCl, and ultrasonic influences.

3.2 Theoretical approach

3.2.1 Chemical reactions

The same as Chapter 2.

3.2.2 Kinetic model

For the reaction obeying first-order kinetics, the following equation applies:

$$\frac{dc}{dt} = -k(c - c_{eq}) \quad [3-1]$$

where c is the concentration of a reactant at time t , c_{eq} the equilibrium concentration, and k the rate constant. Equation [3-1] can be rewritten as,

$$\ln(c - c_{eq}) = -kt + \ln(c_0 - c_{eq}) \quad [3-2]$$

Using Equation [3-2], one can determine k by fitting the plot $\ln(c - c_{eq})$ vs t .

3.2.3 The temperature dependence of rate constants

Chemical reaction rates increase exponentially with temperature, which is frequently expressed by means of the Arrhenius equation:

$$k = A \exp\left(-\frac{E_a}{RT}\right) \quad [3-3]$$

where A is the pre-exponential factor, E_a the activation energy, R the universal gas constant, and T the absolute temperature.

Assuming that both A and E_a are constants, one can obtain the following equation:

$$\frac{d \ln k}{d(1/T)} = -\frac{E_a}{R} \quad [3-4]$$

The activation energy of the reaction of interest could be determined by plotting $\ln k$ vs. $1/T$. A straight line with slope $-E_a/R$ should be obtained on this plot.

3.3 Experiment

The materials and experimental procedures were the same as detailed in Chapter 2 unless otherwise noted.

3.4 Results and discussion

3.4.1 Effect of stirring speed

The effects of stirring speed on the kinetics of nesquehonite precipitation should not be overlooked due to the precipitates and CO₂ gas formed in Step 2. Figure 3.1 shows the change in Mg²⁺ ion concentration during nesquehonite precipitation at different stirring speeds. The initial solution pH was 6.9 and the temperature of the solution was maintained at a constant 40 °C without aeration. The faster the Mg²⁺ ion concentration decreased, the faster the kinetics of nesquehonite precipitation proceeded. As shown in Figure 3.1, the higher the stirring speed, the faster the level of Mg²⁺ ion concentration decreased. Thus, it is very likely that the higher stirring speed improves the diffusion of the precipitates and CO₂ gas formed in Step 2. The increased stirring speed also causes the gas bubbles to become smaller and more likely to overflow from the reaction sites, thereby accelerating the precipitation reaction.

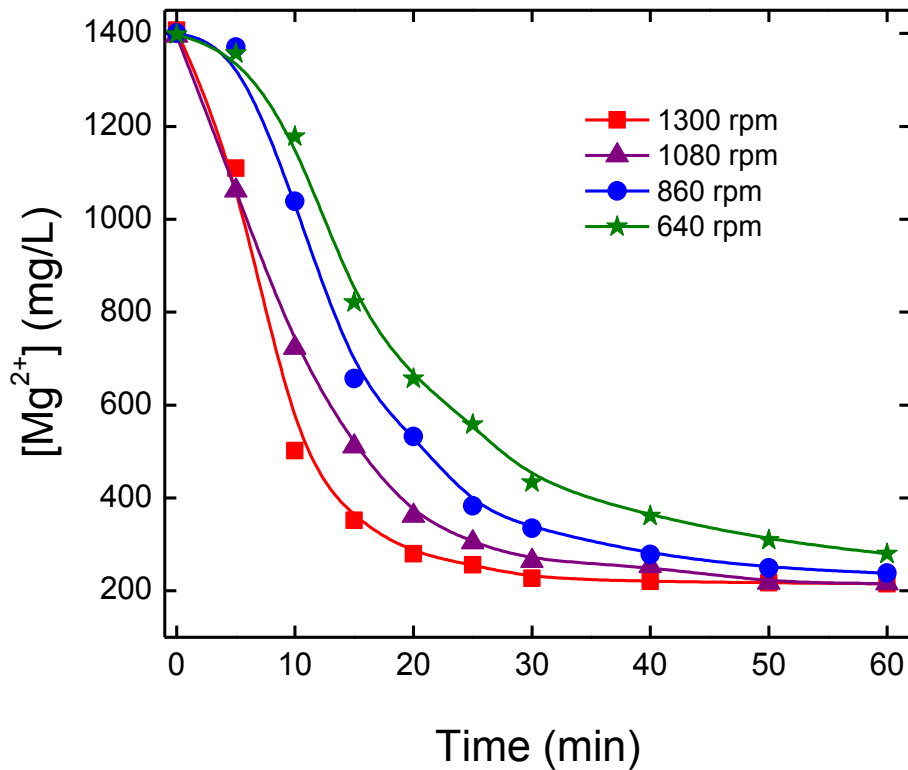


Figure 3.1 The effect of stirring speed on nesquehonite precipitation.

3.4.2 Effect of aeration

Figure 3.2 shows the effect of aeration on nesquehonite precipitation. Two experiments were conducted at 40 °C and at a stirring speed of 640 rpm—with aeration at 10 L/min, and in the absence of aeration. As shown, aeration significantly increased the kinetics of nesquehonite precipitation since air can replace CO₂ and help remove CO₂ from the solution.

Aeration is not a new technique. Many investigators^{1,2,11} have used aeration experimentally to synthesize nesquehonite. Additionally, aeration is a common industrial method for removing CO₂.

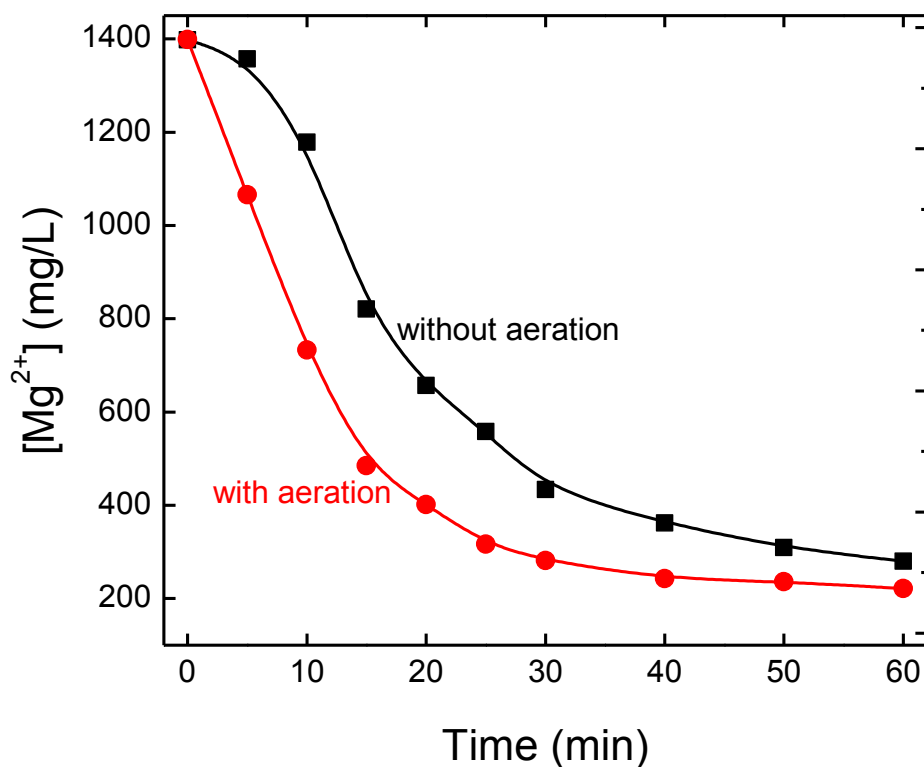


Figure 3.2 The effect of aeration on nesquehonite precipitation.

3.4.3 Effect of NaCl additive

Sodium chloride (NaCl) is the main salt in seawater. Therefore, if sea water is to provide the magnesium source for CO₂ mineralization, the kinetic effects of incorporating NaCl into nesquehonite precipitation should be investigated. Figure 3.3 shows the effect of adding NaCl to the solution on the precipitation of nesquehonite. Two comparative experiments were conducted at 40°C and at a stirring speed of 1080 rpm. In the first, 0.43 M NaCl was added to the solution; in the second, no NaCl was added to the precipitation. As shown, the addition of NaCl slowed down the nesquehonite precipitation to a small extent. The possible reason for this is that the addition of NaCl increases the solubility of nesquehonite. Dong et al.¹² studied the solubility of nesquehonite in NaCl solutions and found that it increased with increasing the concentration of NaCl until the concentration of NaCl reached 2.5M. Cheng et al.⁶ also studied the effect of NaCl on the nucleation kinetics of nesquehonite and reported analogous results; namely, that the activation energy for the reaction of nesquehonite precipitation with the addition of NaCl (78.5 kJ/mol) was higher than without adding NaCl (69.8 kJ/mol)⁶.

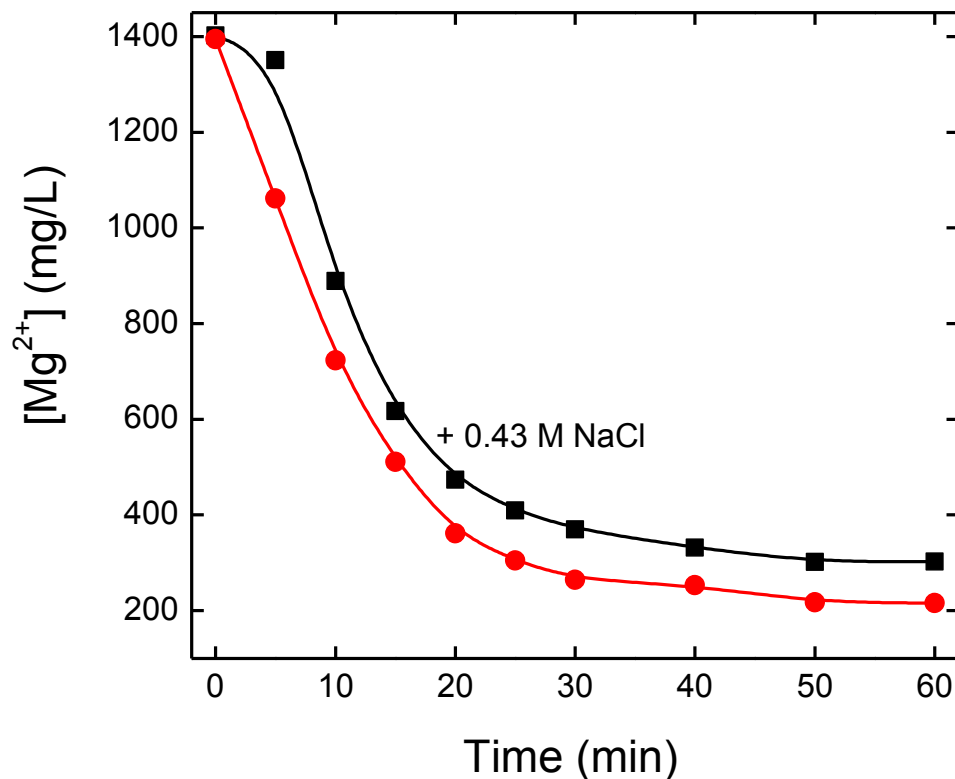


Figure 3.3 The effect of NaCl on nesquehonite precipitation.

3.4.4 Effect of ultrasonic

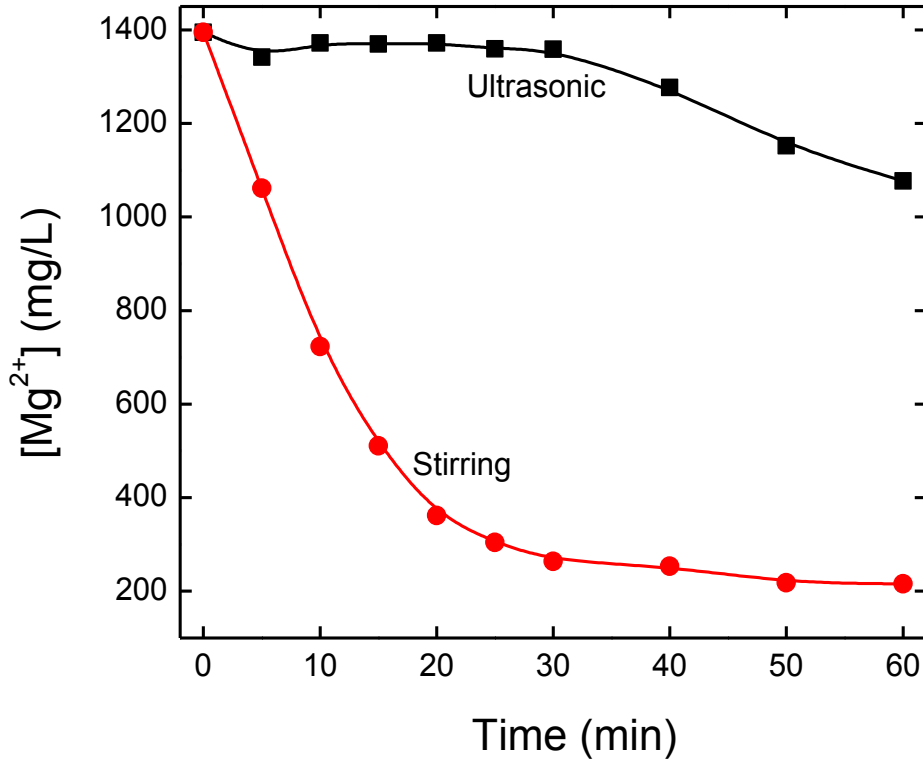


Figure 3.4 The effect of ultrasonic on nesquehonite precipitation.

Figure 3.4 shows the effect of ultrasonic treatment on the precipitation of nesquehonite. Both experiments were carried out at 40 °C. In the first, the nesquehonite precipitation was agitated at 1080 rpm, while for the second, the solution was ultrasonicated using a ultrasonic probe. As shown in the figure, the kinetics of the nesquehonite precipitation was very slow when the ultrasonic treatment was applied. The results were not what we expected probably due to the small energy dissipation rate.

3.4.5 Effect of temperature

The temperature range for the formation of nesquehonite was found to be $< 50\text{ }^{\circ}\text{C}^5$; therefore, the temperature investigated in this study were 20, 30, and 40 $^{\circ}\text{C}$. Experiments were conducted at an initial pH of 6.9, a stirring speed of 640 rpm, and an aerating rate of 10 L/min. In order to determine the rate constants at different temperatures, the Mg^{2+} ion concentration was measured using standard EDTA titration at various time intervals. First-order kinetics was assumed and the rate constants were determined by fitting Mg^{2+} ion concentration using Equation [3-2], as shown in Figure 3.5. It should be noted that we only used the data collected during the initial part of the reaction (prior to reaching equilibrium) to fit the model because the proper fit of Equation [3-2] assumes minimal reverse reaction. The linear plots in Figure 3.5 confirm two findings: (i) the reaction of nesquehonite precipitation is indeed a first-order reaction; (ii) the rate of the reaction increased with increasing temperature, as indicated by the increase in the first-order rate constants (0.016, 0.041, and 0.087 min^{-1} at temperature 20, 30, and 40 $^{\circ}\text{C}$, respectively). The latter finding agreed well with the Arrhenius Equation [3-3], as well as with Cheng's findings⁶. In summary, by increasing the temperature, we were able to accelerate the reaction of nesquehonite precipitation by decreasing the induction time period.

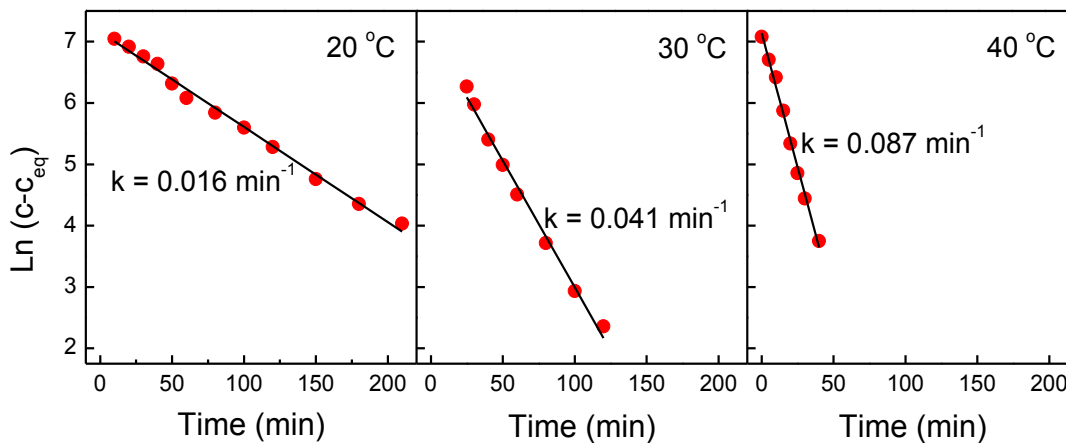


Figure 3.5 The first-order kinetic plots for nesquehonite precipitation at 20, 30, 40 $^{\circ}\text{C}$.

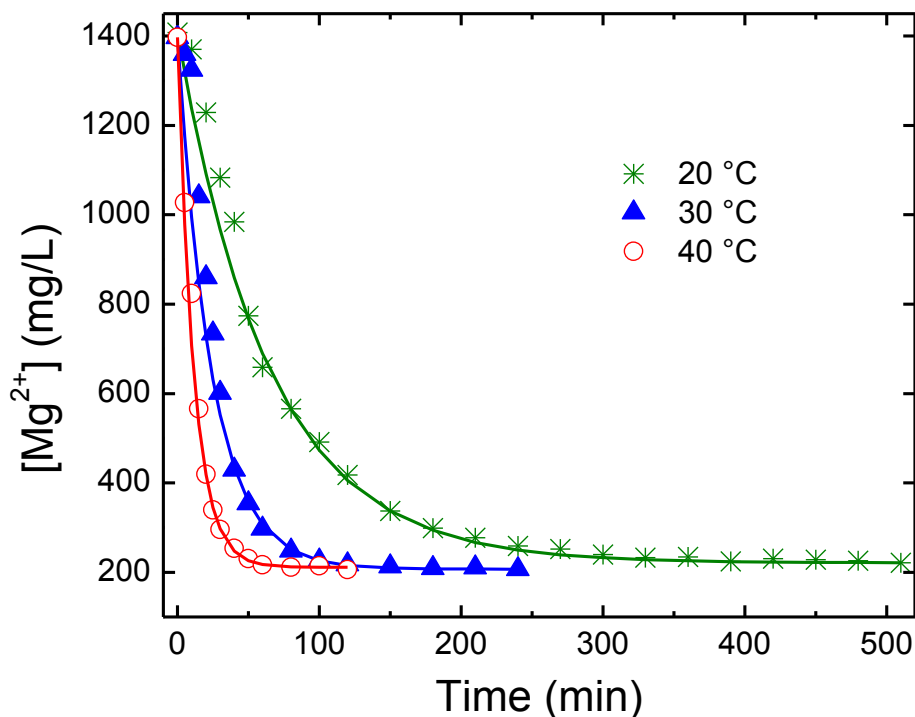


Figure 3.6 Measured Mg^{2+} ion concentration data and first-order model data during nesquehonite precipitation at 20, 30, 40 °C. The solid lines represent modelling data at corresponding temperature using Equation [3-2].

Using the rate constants we obtained, we were able to successfully model the Mg^{2+} ion concentration at different time during nesquehonite precipitation. Figure 3.6 depicts both the measured and modeling data for Mg^{2+} ion concentration. As shown, there was good agreement between the two. This figure also confirms that the Mg^{2+} ion decreased faster at higher temperatures.

We also determined the activation energy (E_a) of the reaction of nesquehonite precipitation by plotting $\ln k$ vs. $1/T$ according to Equation [3-4], using the values of the rate constants obtained from Figure 3.5. The Arrhenius plot is shown in Figure 3.7. The slope of the Arrhenius plot gave us $E_a = 64.6$ kJ/mol, which is in good agreement with the work by Cheng et al.⁶ who found the activation energy for nesquehonite nucleation was 69.8 kJ/mol. The large activation energy result obtained in the present work provides a rationale for the slow kinetics

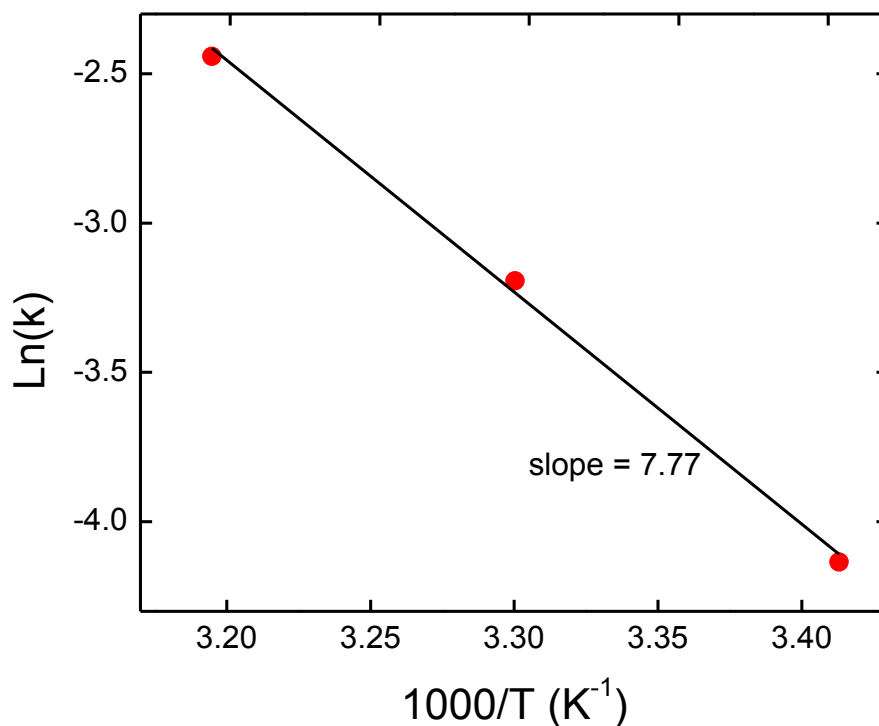


Figure 3.7 Arrhenius plot for nesquehonite precipitation.

observed during nesquehonite precipitation at ambient temperature, which may be attributed to the fact that Mg^{2+} ions are highly hydrated in solution^{13,14}.

Magnesium, belonging to the second group of the periodic table, has a highly ionic character. According to the studies by Bol et al.¹⁵, Mg^{2+} ion possesses strongly bonded layers of water dipoles, having a clear-cut shell of 6 neighboring water molecules in primary hydration and another shell of about 12 water molecules in secondary hydration, which is attributed to the high ratio between the electrical charge and the ion surface area of Mg^{2+} . During the formation of nesquehonite, these water dipoles, having strong electrostatic interaction with all ions, form a barrier around Mg^{2+} ions and are easily incorporated into the carbonate structure.

3.4.6 Effect of pH

Figure 3.8 shows the changes in Mg^{2+} concentration during nesquehonite precipitation at various initial solution pH levels in Step 2. As shown in this figure, the pH level had a significant kinetic effect on the nesquehonite precipitation. Specifically, as the pH increased from 6.6 to 7.2, the kinetics of nesquehonite precipitation increased. As the pH was further increased to 7.5, the kinetics didn't change while the Mg^{2+} ion concentration left in the solution after reaction increased.

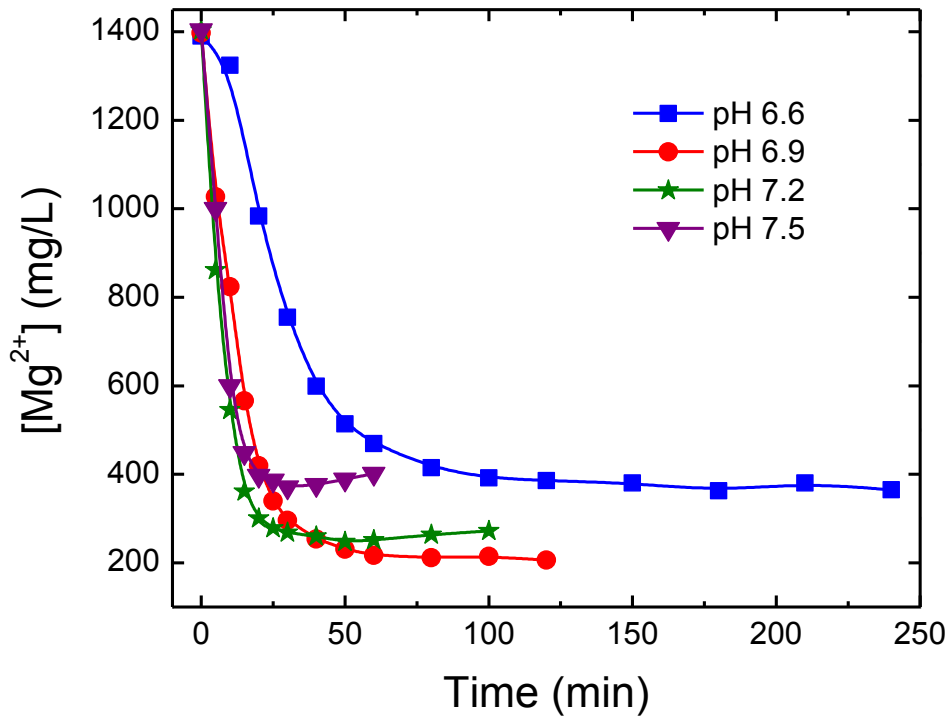


Figure 3.8 pH effect on nesquehonite precipitation.

The % reduction of Mg^{2+} ion at different pH levels and at two time intervals (30 min and 1 h) was also calculated, as shown in Figure 3.9. The % reduction of Mg^{2+} ion increased with pH, reaching a maximum at pH 7, and then decreased.

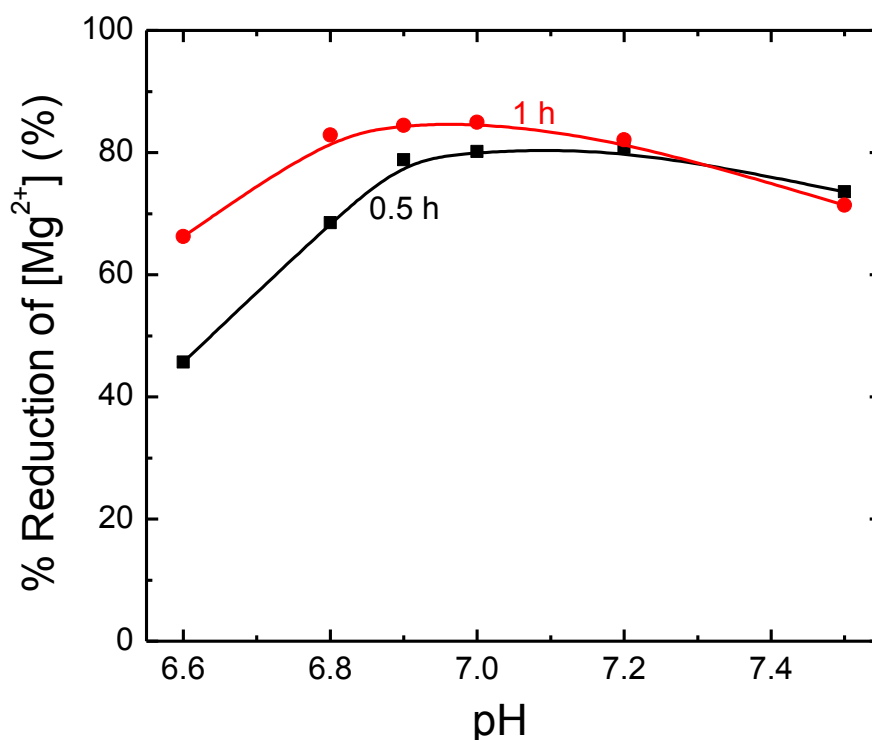
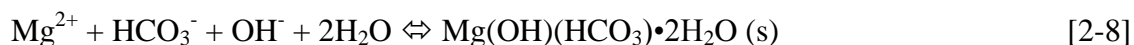


Figure 3.9 % Reduction of Mg^{2+} ion at different pHs at reaction times of 30 min and 1 h.

It's important to note that the initial solution pH for nesquehonite precipitation in Step 2 is also the equilibrium pH of CO_2 dissolution in Step 1. From the thermodynamic calculations listed in Chapter 2, we know that in a closed system dissolved CO_2 ($\text{CO}_2(\text{aq})$) and carbonic acid (H_2CO_3) predominate at low pH levels, bicarbonate ions (HCO_3^-) dominate at mid-range pH levels, and carbonate ions (CO_3^{2-}) dominate at high pH levels. In the initial solution pH range applied in this study (6.6–7.5), HCO_3^- ions were the dominant species (Figure 2.1). We also know that regardless of the amount of CO_2 gas that is injected into the solution, both the HCO_3^- ion concentration and the total carbonic species concentration increase with increasing equilibrium pH levels (Figure 2.2). In addition, the OH^- ion concentration increases with increasing pH.

Two forces related to the effect of pH are shown to impact the precipitation of nesquehonite. The first force is that the concentrations of HCO_3^- and OH^- ions in the solution

increase with increasing solution pH levels, thereby facilitating the precipitation of nesquehonite according to the chemical reaction discussed in Chapter 2, and shown below:



The second force is that the total concentration of ionic species present in the solution also increases with rising solution pH levels, which subsequently amplifies the ionic strength of the solution, resulting in enhanced nesquehonite solubility. The possible reason for this could be that the higher ionic strength leads to the increase in the size and density of ion bodies in the solution, which thus increases the distance between cationic (Mg^{2+} ions) and anionic (HCO_3^- and OH^- ions) ions and thus hinders the combination of the two.

These two forces, however, are in conflict. When we increased the pH from 6.6 to 7.2, the first force dominated; when the pH was further increased to 7.5, the second force dominated.

Soong and Druckenmiller^{9,10,16} studied the pH effects on calcite precipitation by reacting CO_2 gas with brine samples; the researchers confirmed that the pH must be basic for calcite precipitation. Unlike calcite precipitation, nesquehonite precipitation could occur at neutral initial pH levels. However, it must be noted that the solution pH increased over time during nesquehonite precipitation, as described in Chapter 2.

3.4.7 Characterization of solid products

The solid products obtained under different experimental conditions were characterized by measuring their XRD patterns. As shown in Figure 3.10, the XRD patterns of all the solid products were in good agreement with the XRD pattern for nesquehonite.

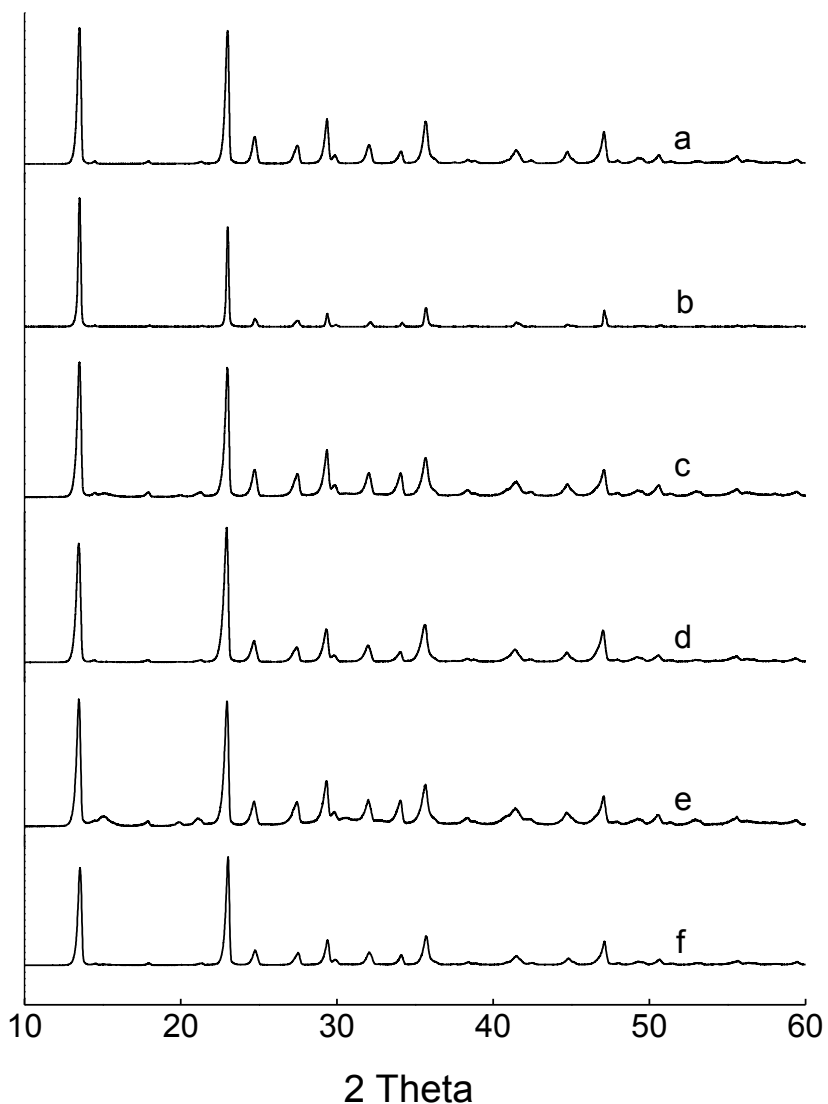


Figure 3.10 XRD pattern of the solid products under different experimental conditions. (a) 20 °C, pH 6.9; (b) 30 °C, pH 6.9; (c) 40 °C, pH 6.9; (d) 40 °C, pH 6.6; (e) 40 °C, pH 7.2; (f) 40 °C, pH 7.5.

3.5 Conclusions

The reaction kinetics associated with the precipitation of nesquehonite were studied by measuring the Mg^{2+} ion concentration in solution at different time intervals. The effects of stirring speed, aeration, additive NaCl, ultrasonic treatment, temperature and initial solution pH were investigated. The following conclusions resulted from our studies:

- 1) Higher stirring speed and aeration can improve the kinetics of nesquehonite precipitation.
- 2) The addition of NaCl and ultrasonic treatment slow down the precipitation of nesquehonite.
- 3) Temperature significantly accelerates the kinetic activity of nesquehonite precipitation. Specifically, the rate constants were determined to be 0.016, 0.041, and 0.087 min⁻¹ at temperatures of 20, 30, and 40 °C, respectively. The activation energy of the nesquehonite precipitation reaction was calculated to be 64.6 kJ/mol.
- 4) A first-order kinetic model was developed to successfully predict the Mg²⁺ ion concentration during nesquehonite precipitation at different temperatures. There was a good agreement between measured and predicted data.
- 5) The initial pH of the solution also has a significant kinetic effect on the precipitation of nesquehonite. The optimum initial solution pH for nesquehonite precipitation was determined to be 7.

3.6 References

1. Davies, P.J. and B. Bubela, *The transformation of nesquehonite into hydromagnesite*. Chemical Geology, 1973. **12**(4): p. 289-300.
2. Ming, D.W. and W.T. Franklin, *Synthesis and Characterization of Lansfordite and Nesquehonite*. Soil Sci. Soc. Am. J. **49**(5): p. 1303-1308.
3. Klopogge, J.T., et al., *Low temperature synthesis and characterization of nesquehonite*. Journal of Materials Science Letters, 2003. **22**(11): p. 825-829.
4. Hänchen, M., et al., *Precipitation in the Mg-carbonate system--effects of temperature and CO₂ pressure*. Chemical Engineering Science, 2008. **63**(4): p. 1012-1028.
5. Cheng, W., Z. Li, and G.P. Demopoulos, *Effects of Temperature on the Preparation of Magnesium Carbonate Hydrates by Reaction of MgCl₂ with Na₂CO₃*. Chinese Journal of Chemical Engineering, 2009. **17**(4): p. 661-666.
6. Cheng, W. and Z. Li, *Nucleation kinetics of nesquehonite (MgCO₃·3H₂O) in the MgCl₂-Na₂CO₃ system*. Journal of Crystal Growth, 2010. **312**(9): p. 1563-1571.
7. Wang, Y., Z. Li, and G.P. Demopoulos, *Controlled precipitation of nesquehonite (MgCO₃·3H₂O) by the reaction of MgCl₂ with (NH₄)₂CO₃*. Journal of Crystal Growth, 2008. **310**(6): p. 1220-1227.
8. Ferrini, V., C. De Vito, and S. Mignardi, *Synthesis of nesquehonite by reaction of gaseous CO₂ with Mg chloride solution: Its potential role in the sequestration of carbon dioxide*. Journal of Hazardous Materials, 2009. **168**(2-3): p. 832-837.

9. Soong, Y., et al., *Experimental and simulation studies on mineral trapping of CO₂ with brine*. Energy Conversion and Management, 2004. **45**(11): p. 1845-1859.
10. Druckenmiller, M.L. and M.M. Maroto-Valer, *Carbon sequestration using brine of adjusted pH to form mineral carbonates*. Fuel processing technology, 2005. **86**(14-15): p. 1599-1614.
11. Kazakov, A., M. Tikhomirova, and V. Plotnikova, *The system of carbonate equilibria*. International Geology Review, 1959. **1**(10): p. 1-39.
12. Dong, M., et al., *Solubility and stability of nesquehonite (MgCO₃·3H₂O) in NaCl, KCl, MgCl₂, and NH₄Cl solutions*. Journal of Chemical & Engineering Data, 2008. **53**(11): p. 2586-2593.
13. Sayles, F. and W. Fyfe, *The crystallization of magnesite from aqueous solution*. Geochimica et Cosmochimica Acta, 1973. **37**(1): p. 87-96, IN1-IN2, 97-99.
14. Deelman, J., *Breaking Ostwald's rule*. Chemie der Erde Geochemistry, 2001. **61**(3): p. 224-235.
15. Bol, W., G. Gerrits, and C. van Panthaleon Eck, *The hydration of divalent cations in aqueous solution. An X-ray investigation with isomorphous replacement*. Journal of Applied Crystallography, 1970. **3**(6): p. 486-492.
16. Soong, Y., et al., *CO₂ sequestration with brine solution and fly ashes*. Energy Conversion and Management, 2006. **47**(13): p. 1676-1685.

Chapter 4

CO₂ Mineralization Using Ca²⁺ Ions Alone and Using Mg²⁺ and Ca²⁺ Ions Together

4.1 Introduction

Several reactive metal ions such as Mg²⁺, Ca²⁺, Fe²⁺ and Fe³⁺ ions can be potentially used to mineralize CO₂ gas for sequestration because of the thermodynamic stability of their carbonate products. Mg²⁺ and Ca²⁺ ions are most important because their high concentrations in the sea water and produced water. We have studied the process of CO₂ mineralization using Mg²⁺ ions alone in previous chapters. In this chapter, we focus on the CO₂ mineralization using Ca²⁺ ions in isolation and using Mg²⁺ and Ca²⁺ ions in tandem.

4.1.1 CO₂ mineralization using Ca²⁺ ions alone

Produced water generated from oil and gas industries has high concentration of Ca²⁺ ions, as shown in table 1.1. Sea water also contains 400 mg/L Ca²⁺ ions on average. The Ca²⁺ ions from these solutions could react with CO₂ gas to produce environmentally benign and chemically stable calcium carbonate (CaCO₃) that would safely and permanently store CO₂. CaCO₃ commonly occurs as rocks and sediments in nature in marine settings all over the world. It is also the main component of shells or skeletons of marine animals and plants. Over geologic time, the natural massive formation of CaCO₃ based on the dissolution of CO₂ in oceans has played an important role in balancing the world's carbon cycle.

The carbonate mineral obtained from the CO₂ mineralization process—calcium carbonate—can be used in a variety of industries. First, it could be applied in the construction industry as a building material or limestone aggregate for road building, as an ingredient of cement, or as the starting material for the preparation of lime. Second, it could also be used in paper industry for paper coating or as a filler due to its cheaper price than the wood fiber. In addition, calcium carbonate is a popular filler in plastics application, to improve the tensile strength, the elongation, and the volume resistivity of polyvinyl chloride cables or to increase rigidity of polypropylene. Furthermore, precipitated calcium carbonate could be used as a white paint. Other applications of calcium carbonate include formation-bridging agents in the drilling

fluids in the oil industry, adding material for a wide range of adhesives, and dietary calcium supplement in health application.

4.1.2 CO₂ mineralization using Mg²⁺ and Ca²⁺ ions together

CO₂ gas can also react with both Mg²⁺ and Ca²⁺ ions to form dolomite (CaMg(CO₃)₂), which is an important sedimentary and metamorphic mineral found in dolostones and metadolostones. Dolomite naturally occurs in deep-sea sediments, highly saline lakes, and even caves.

Table 4.1 shows the standard gibbs free energy of the formation of selected calcium/magnesium carbonates. As shown, the standard Gibbs free energy of formation ($\Delta_f G^\circ$) of dolomite is -2161.7 kJ/mol, much lower than those for other selected minerals. Therefore, dolomite may be more thermodynamically stable and more readily formed than the rest. In this chapter, the feasibility of dolomitization as a means of CO₂ mineralization for sequestration was studied.

Table 4.1 The Gibbs free energy of the formation of selected Ca/Mg-carbonate

Mineral	Composition	$\Delta_f G_{298}^\circ$ (kJ/mol)	Reference
Nesquehonite	MgCO ₃ •3H ₂ O	-1723.8	Robie and Hemingway (1995) ¹
Aragonite	CaCO ₃	-1128.3	Hummel et al. (2002) ²
Calcite	CaCO ₃	-1129.1	Hummel et al. (2002) ²
monohydrocalcite	CaCO ₃ •H ₂ O	-1361.6	Robie and Hemingway (1995) ¹
Dolomite (disordered)	CaMg(CO ₃) ₂	-2158.4	Woods and Garrels (1987) ³
Dolomite (ordered)	CaMg(CO ₃) ₂	-2161.7	Woods and Garrels (1987) ³

4.1.3 Chemical reaction

CO₂ mineralization using Ca²⁺ ions alone and using Mg²⁺ and Ca²⁺ ions together may occur via the chemical Reactions [4-1] to [4-7] as shown below. CO₂ gas dissolves into water (Reaction [4-1]). Then carbonic acid (Reaction [4-2]) forms, which then dissociates into bicarbonate (Reaction [4-3]) and carbonate ions (Reaction [4-5]). Dissolved CO₂ can also react

with hydroxide ions (OH^-) to form bicarbonate ions (Reaction [4-4]). Then Ca^{2+} ions alone (Reaction [4-6]) or Mg^{2+} and Ca^{2+} ions together (Reaction [4-7]) react with carbonate ions to form the mineral calcite or dolomite, respectively.



4.2 Experiment

4.2.1 Materials

Anhydrous MgCl_2 (99%, Alfa Aesar) provided a source of magnesium, and anhydrous CaCl_2 (Granular 4-20 mesh, Fisher Science) provided a source of calcium. Compressed CO_2 gas (Bone Dry Grade, Airgas), and 10 N standardized NaOH solution as a pH controller, were used in our experiments. Dihydrated ethylenediaminetetraacetic acid disodium salt ($\text{Na}_2\text{H}_2\text{EDTA} \cdot 2\text{H}_2\text{O}$, 99+%, Alfa Aesar), pure Eriochrome Black T (EBT, indicator grade, Acros Organics), 2-methoxyethanol (ACS, 99.3+%, Alfa Aesar) and ammonia buffer solution pH 10 (Sigma-Aldrich) were used for standard EDTA titration. All experimental work for solution preparation, dilution, apparatus washing, etc. was done using the deionized Millipore water with a resistivity of 18.2 $\text{M}\Omega/\text{cm}$, which was obtained using a Direct-Q3 water purification system.

4.2.2 Procedure

When only Ca^{2+} ions were studied in CO_2 mineralization process, CaCl_2 solution with a Ca^{2+} ion concentration of 400 mg/L (average Ca^{2+} ion concentration in sea water) was applied in the experiment. When both Mg^{2+} and Ca^{2+} ions were present in the solution, a mixture of MgCl_2 and CaCl_2 solution was used, with a Mg^{2+} ion concentration of 1400 mg/L and Ca^{2+} ion concentration of 400 mg/L. The other procedures were the same as described in Chapter 2.

4.3 Results and Discussion

4.3.1 CO₂ mineralization using Ca²⁺ ions alone

After CO₂ was injected into the solution containing 400 mg/L Ca²⁺ ions, the solution pH decreased fast. In order to increase pH, diluted solution of NaOH was added into the solution dropwise. Immediately after NaOH solution was added, white precipitates formed in the solution. If more CO₂ gas was injected, the precipitates dissolved due to the formation of HCO₃⁻ ions.

Our experimental results show that when Ca²⁺ ions alone were applied in CO₂ mineralization, the precipitation from the aqueous solution proceeded very fast. However, as we showed in Chapter 2 and Chapter 3, when Mg²⁺ ions alone were applied under ambient conditions, the precipitation from the solution was very slow. It may be attributed to the fact that although both calcium and magnesium belong to the second group of the periodic table, Mg²⁺ ion is more strongly hydrated in water than Ca²⁺ ion, which in turn can be attributed to the difference in ionic radii involved. The ionic radius of the 6-coordinated Mg²⁺ ions is 0.72 Å, while that of Ca²⁺ ions is 1.0 Å⁴. Therefore, the activation energy required to displace the water molecules from the hydrated Mg²⁺ ions would be higher than from the hydrated Ca²⁺ ions, as shown in table 4.2.

Table 4.2 Radius, cation-O distance and water binding energy for Mg/Ca complex⁵

Complex	Cation radius (Å)	Cation-O distance (Å)	Water binding energy (ΔE) (Kcal/mol)
[Mg(H ₂ O) ₆] ²⁺	0.65	2.08	303.9
[Mg(H ₂ O) ₆](H ₂ O) ₁₂ ²⁺	0.65	2.07	460.8
[Ca(H ₂ O) ₆] ²⁺	0.99	2.37	234.4
[Ca(H ₂ O) ₆](H ₂ O) ₁₂ ²⁺	0.99	2.35	389.2

Another possible reason for faster kinetics associated in the precipitation of calcium carbonate mineral than magnesium carbonate mineral could be the difference in the solubility of

the two minerals. Table 4.3 shows the solubility product of calcium and magnesium carbonate at 25 °C, indicating that calcium carbonate is far less soluble than magnesium carbonate.

Table 4.3 Solubility product of selected calcium/magnesium mineral⁶

Compound	Formula	K_{sp} (at 25 °C)
Calcium carbonate (calcite)	CaCO_3	3.36×10^{-9}
Calcium carbonate (aragonite)	CaCO_3	6.0×10^{-9}
Magnesium carbonate	MgCO_3	6.82×10^{-6}

4.3.2 CO_2 mineralization using Mg^{2+} and Ca^{2+} ions together

Figure 4.1 shows the total concentration of Mg^{2+} and Ca^{2+} ions in the solution at different times. As shown, the total concentration of Mg^{2+} and Ca^{2+} ions in the solution decreased with time due to the formation of the solid product and then reached its minimum.

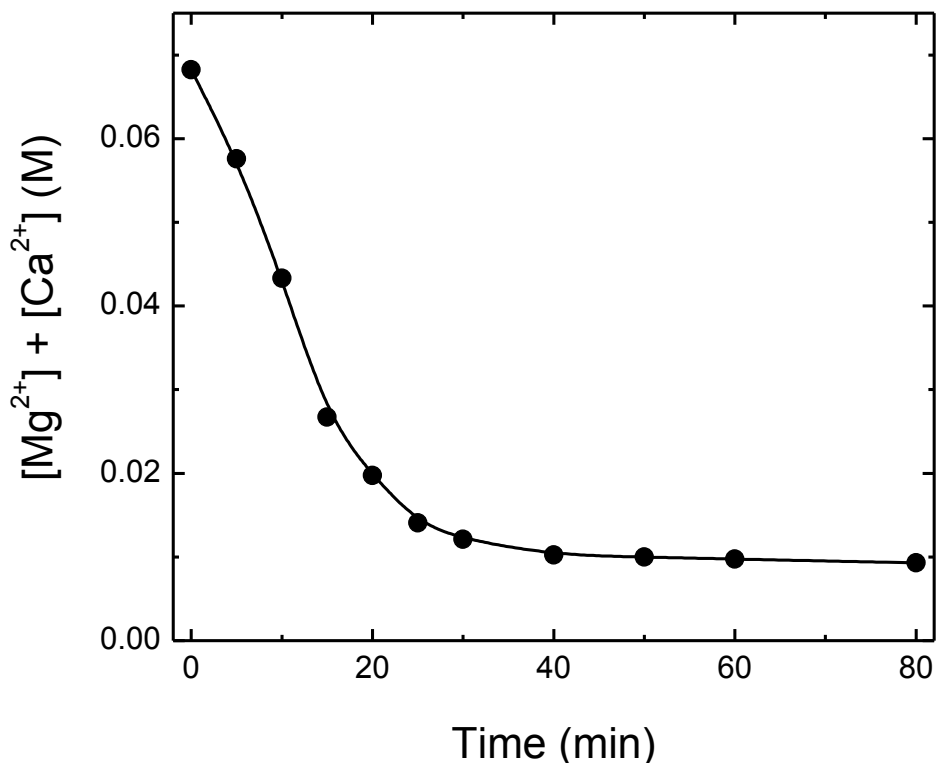


Figure 4.1 Change in the sum of Mg^{2+} and Ca^{2+} ion concentration during the precipitation of solid products.

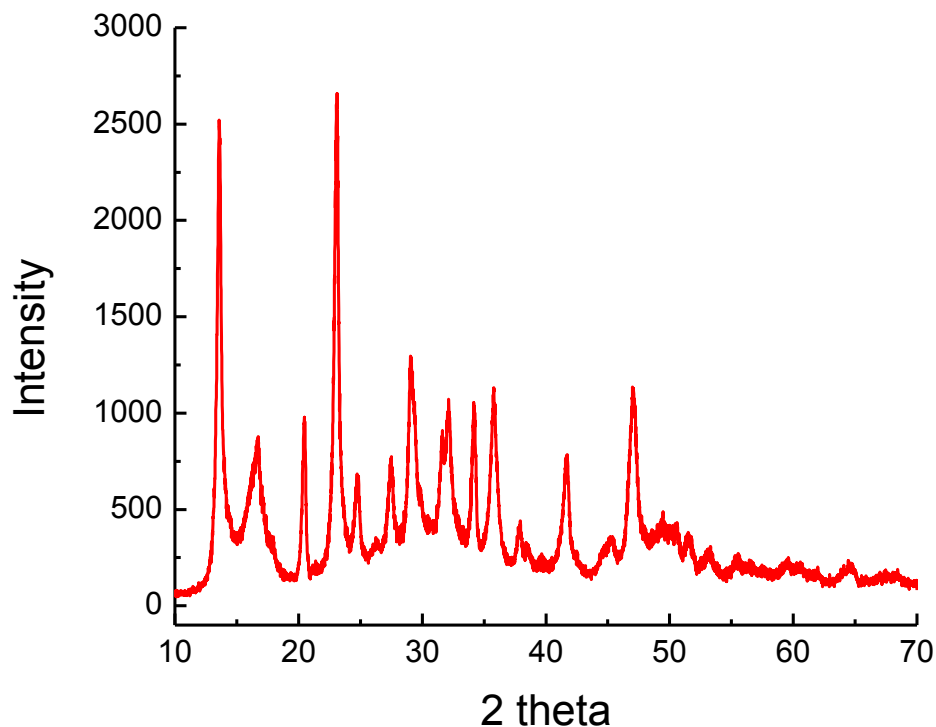


Figure 4.2 The XRD pattern of the solid product.

Figure 4.2 shows the XRD pattern of the solid product. Clearly, it was not dolomite. By analyzing the x-ray diffraction patterns, we concluded that the solid product was a mixture of nesquehonite ($\text{Mg}(\text{OH})(\text{HCO}_3) \cdot 2\text{H}_2\text{O}$) and monohydrocalcite ($\text{CaCO}_3 \cdot \text{H}_2\text{O}$).

The failure of the formation of dolomite may be attributed to the slow kinetics of dolomitization. Although dolomite can form at relatively low temperature in nature, the laboratory synthesis of dolomite at room temperature has not been successful. The lowest temperature of dolomitization reported in the laboratory was 60 °C by Usdowski⁷. However, it took 7 years to complete the reaction. Usdowski suggested that it is possible that dolomitization may occur at 30 °C in nature within a long time period of 10^2 to 10^3 years. At higher temperatures, the reaction rate is increased. Gains⁸ carried out dolomite synthesis at 100 °C, which took 300 hours (using Li_2CO_3) or 400 hours (using Na_2CO_3) to complete the dolomitization.

4.4 Conclusions

In this chapter, we studied the feasibilities of using Ca^{2+} ions alone and both Mg^{2+} and Ca^{2+} ions together to mineralize CO_2 gas for sequestration. We have the following conclusions:

- 1) When Ca^{2+} ions were used alone for CO_2 mineralization, the precipitation of carbonate mineral was fast.
- 2) It's not viable to form dolomite using both Mg^{2+} and Ca^{2+} ions as an approach of CO_2 mineralization due to the slow kinetics of dolomitization.

4.5 References

1. Robie, R.A. and B.S. Hemingway, Thermodynamic properties of minerals and related substances at 298.15 K and 1 bar (10^5 Pascals) pressure and at higher temperatures. US Geol. Survey Bull., vol. 2131, p. 461-461 (1995). 1995. 2131: p. 461-461.
2. Hummel, W., et al., Nagra/PSI chemical thermodynamic data base 01/01. 2002: Universal-Publishers.
3. Woods, T.L. and R.M. Garrels, Thermodynamic values at low temperature for natural inorganic materials. 1987: Oxford univ. press New York; Oxford.
4. Shannon, R., Revised effective ionic radii and systematic studies of interatomic distances in halides and chalcogenides. Acta Crystallographica Section A: Crystal Physics, Diffraction, Theoretical and General Crystallography, 1976. 32(5): p. 751-767.
5. Pavlov, M., P.E.M. Siegbahn, and M. Sandström, Hydration of beryllium, magnesium, calcium, and zinc ions using density functional theory. The Journal of Physical Chemistry A, 1998. 102(1): p. 219-228.
6. Lide, D.R., CRC handbook of chemistry and physics. 2004: CRC Pr I Llc.
7. Usdowski, E., Synthesis of dolomite and magnesite at 60 °C in the system Ca^{2+} - Mg^{2+} - CO_3^{2-} - Cl_2^{2-} - H_2O . Naturwissenschaften, 1989. 76(8): p. 374-375.
8. Gaines, A.M., Protodolomite synthesis at 100 °C and atmospheric pressure. Science, 1974. 183(4124): p. 518-520.

Chapter 5

Conclusions and Future Work

5.1 Conclusions

In the present work, possibility of mineralizing CO₂ with the reactive species such as Mg²⁺ and Ca²⁺ ions present sea water was investigated. Batch experiments were conducted by injecting gaseous CO₂ into solutions containing 1400 ppm of Mg²⁺ and/or 400 ppm of Ca²⁺ ions. Based on the experimental results of the present work, the following conclusions may be drawn:

- 1) The CO₂ mineralization process developed in the present work is feasible both kinetically and energetically, and safe; and affords a long-term sequestration of CO₂.
- 2) When Mg²⁺ ions alone were used for CO₂ mineralization, the solid product of this process was indentified to be nesquehonite as determined by using XRD, SEM, EDS technologies. Under nearly ambient conditions (40 °C and atmospheric pressure), as much as 86% of the magnesium ions reacted with CO₂ in one hour.
- 3) Effects of various operating parameters on the kinetics of nesquehonite formation were also studied under various conditions. The parameters studied included stirring speed, aeration, additive NaCl, ultrasonic, temperature, and pH. Of these, temperature and initial solution pH were found to have the most significant effects on the kinetics of nesquehonite precipitation. The rate constants were 0.016, 0.041, and 0.087 min⁻¹ at temperature 20, 30, and 40 °C, respectively. The activation energy for the nesquehonite precipitation was calculated to be 64.6 kJ/mol. The kinetics increased with increasing pH, reaching a maximum at pH 7 and then decreasing with a further increase in pH.
- 4) A first-order kinetic model was developed to successfully predict the Mg²⁺ ion concentration during the period of nesquehonite precipitation at different temperatures.
- 5) CO₂ mineralized more readily in Ca²⁺ ion solutions than Mg²⁺ solutions. However, it was not possible to form dolomite by reacting CO₂ in a solution containing both Mg²⁺ and Ca²⁺ ions.

5.2 Future Work

Although this CO₂ mineralization process is proved to be chemically feasible and suitable for safe and long-term storage, there's a big concern about this process. As shown in chapter 2, the solution pH decreases with time if CO₂ is injected into the solution, resulting the acidization of the solution in Step 1, which is considered as the concern that will likely turn down this process. Therefore, the future work would focus on the neutralization of the solution. The recommendations are shown below:

- 1) Cheap natural alkaline minerals such as limestone, olivine could potentially be used to prevent the acidization of the solution based on the minimum solubility theory. Experiments are highly recommended to improve the kinetics of the dissolution of the minerals, such as the effect of particle size and temperature.
- 2) Studies on using alkaline industrial wastes such as steel slags, fly ashes, and bauxite residues to increase the pH of the solution for CO₂ mineralization are also highly recommended. Uses of these wastes could potentially not only improve CO₂ mineralization but also solve environmental problems.
- 3) Experiments using samples of real seawater or produced water are also recommended.
- 4) Cost analysis of the whole process is also recommended before applying it into industrial application.